LC-ESI-HRMS - lipidomics of phospholipids

– Characterization of extraction, chromatography and detection parameters

Katharina M. Rund[1, #], Laura Carpanedo[1, #], Robin Lauterbach[1], Tim Wermund[1], Annette L. West[2],

Luca M. Wende[1], Philip C. Calder[2,3], Nils Helge Schebb[1*]

[1] Chair of Food Chemistry, Faculty of Mathematics and Natural Sciences, University of Wuppertal,

Wuppertal, Germany

[2] School of Human Development and Health, Faculty of Medicine, University of Southampton,

Southampton, United Kingdom

[3] National Institute for Health Research (NIHR) Southampton Biomedical Research Centre,

University Hospital Southampton NHS Foundation Trust and University of Southampton,

Southampton, United Kingdom

# Both authors contributed equally

*Contact information of the corresponding author:

Nils Helge Schebb

Chair of Food Chemistry

Faculty of Mathematics and Natural Sciences

University of Wuppertal

Gaussstr. 20

42119 Wuppertal

nils@schebb-web.de

Tel: +49-202-439-3457

30 **Abstract**

31 Lipids are a diverse class of molecules involved in many biological functions including cell signaling

32 or cell membrane assembly. Owing to this relevance, LC-MS/MS based lipidomics emerged as a major

33 field in modern analytical chemistry. Here, we thoroughly characterized the influence of MS and LC

34 settings – of a Q Exactive HF operated in Full MS/data-dependent MS^2 TOP N acquisition mode - in

35 order to optimize the semi-quantification of polar lipids. Optimization of MS-source settings improved

36 the signal intensity by factor 3 compared to default settings. Polar lipids were separated on an

37 ACQUITY Premier CSH C18 reversed-phase column (100 x 2.1 mm, 1.7 µm, 130 Å) during an elution

38 window of 28 min, leading to a sufficient number of both data points across the chromatographic peaks,

39 as well as MS^2 spectra. Analysis was carried out in positive and negative ionization mode enabling the

40 detection of a broader spectrum of lipids and to support the structural characterization of lipids. Optimal

41 sample preparation of biological samples was achieved by liquid-liquid extraction using MeOH/MTBE

42 resulting in an excellent extraction recovery >85% with an intra-day and inter-day variability <15%.

43 The optimized method was applied on the investigation of changes in the phospholipid pattern in plasma

44 from human subjects supplemented with n3-PUFA (20:5 and 22:6). The strongest increase was

45 observed for lipids bearing 20:5, while 22:4 bearing lipids were lowered. Specifically, LPC 20:5_0:0

46 and PC 16:0_20:5 were found to be strongest elevated, while PE 18:0_22:4 and PC 18:2_18:2 were

47 decreased by n3-PUFA supplementation. These results were confirmed by targeted LC-MS/MS using

48 commercially available phospholipids as standards.

49

50

51

52

53 Abbreviation

54

ACN	acetonitrile
AGC	automatic gain control
ARA	arachidonic acid (20:4(5Z,8Z,11Z,14Z))
CE	collision energy
Chol Ester	cholesteryl ester
CXP	collision cell exit potential
dd	data-dependent
DG	diacylglycerol
DHA	docosahexaenoic acid (22:6(4Z,7Z,10Z,13Z,16Z,19Z))
DP	declustering potential
EDTA	ethylenediaminetetraacetic acid
EPA	eicosapentaenoic acid (20:5(5Z,8Z,11Z,14Z,17Z))
ESI	electrospray ionization
ESI(+)	positive electrospray ionization
ESI(-)	negative electrospray ionization
FC	free cholesterol
FWHM	full width at half maximum
HESI	heated electrospray ionization
HILIC	hydrophilic interaction liquid chromatography
HPLC	high pressure liquid chromatography
HRMS	high resolution mass spectrometry
IPA	*iso*-propanol
IS	internal standard
IT	injection time
LC	liquid chromatography
LLE	liquid-liquid extraction
LLOQ	lower limit of quantification
LOD	limit of detection
LPC	lysophosphatidylcholine
LPE	lysophosphatidylethanolamine
m/z	mass-to-charge ratio
MeOH	methanol
MG	monoacylglycerol
MRM	multiple reaction monitoring
MS	mass spectrometry
MTBE	*tert*-butyl methyl ether
NCE	normalized collision energy
NPLC	normal phase liquid chromatography
PA	phosphatidic acid
PC	phosphatidylcholine
PE	phosphatidylethanolamine
PG	phosphatidylglycerol
PI	phosphatidylinositol
PS	phosphatidylserine
PUFA	polyunsaturated fatty acids

R	resolution
RF	radio frequency
RPLC	reversed phase liquid chromatography
RSD	relative standard deviation
S/N	signal-to-noise ratio
SM	sphingomyelin
sn	stereospecific numbering
SPLASH	single-vial prepared lipidomic analytical standard for human plasma lipids
TG	triacylglycerol
TIC	total ion current
t_R	retention time
XIC	extracted ion chromatogram

55

56

Introduction

57

58

59   Lipids are lipophilic small molecules involved in many biological functions including cell

60   membrane assembly, energy metabolism, cell signaling and regulation of inflammation. They are

61   classified in eight major lipid categories: fatty acids, sphingolipids, glycerolipids,

62   glycerophospholipids, sterol lipids, prenol lipids, saccharolipids and polyketides (1). Fatty acids can be

63   saturated, e.g. stearic acid (18:0), monounsaturated, or polyunsaturated of the n3, n6 or n9 series, e.g.

64   eicosapentaenoic   acid   (EPA,   20:5(5Z,8Z,11Z,14Z,17Z)),   arachidonic   acid   (ARA,

65   20:4(5Z,8Z,11Z,14Z)) or oleic acid (18:1(9Z)) (2). Fatty acids are the major components of

66   phospholipids which are the main constituents of the cellular membrane (3, 4). Driven by the biological

67   importance, lipidomics has emerged as a major field of research in life sciences in the past decades.

68   However, due to the structural diversity of lipids, a simultaneous analysis of "all", i.e., a comprehensive

69   set of lipids in untargeted lipidomics is challenging.

70   Compared to shotgun lipidomics, liquid chromatography coupled to mass spectrometry (LC-

71   MS) allows to separate overlapping isomeric and isobaric lipid species in complex biological matrices

72   (5). The separation of lipids can be carried out by normal phase liquid chromatography (NPLC) and

73   hydrophilic interaction liquid chromatography (HILIC) allowing the separation based on the lipid

74   classes, e.g. by the head group of phospholipids; or by reversed phase liquid chromatography (RPLC)

75   where the separation of the lipids is based on their hydrophobicity, i.e. length of the fatty acyl chains

76 and degree of unsaturation (6). RPLC comprising about 71% of all lipidomics applications has been

77 most widely used for the analysis of complex lipids using C8 (7), C18 (8, 9), or C30 (10) modified silica

78 columns. Criscuolo et al. showed that a C18 column achieved a better separation for polar lipids such

79 as lysophospholipids, sphingomyelin or glycerophospholipids compared to a C30 column (11).

80 Separation of isobaric phospholipid species was previously achieved using C18 columns, e.g.

81 ACQUITY UPLC BEH C18 (12) or ACQUITY Premier CSH C18 (13).

82 For MS detection, untargeted analysis using high resolution and acquisition in Full MS mode

83 is a promising approach as it allows simultaneous and comprehensive monitoring of a broad range of

84 lipids extracted from a biological sample. Additionally, using data-dependent fragmentation, product

85 ion spectra are obtained helping to identify the individual lipid species based on distinct fragmentation

86 behavior. The processing of this huge amount of data generated during untargeted analysis is performed

87 with bioinformatic software in two steps including first peak detection and peak alignment, and

88 subsequent lipid annotation using comprehensive databases (6, 14). Different software packages for the

89 processing of lipid data have been developed and are available open source, as well as commercially

90 (15).

91 Targeted LC-MS/MS analysis only allows the detection of preselected analytes of interest.

92 During method development a focus is set on the optimization of LC and MS parameters, assuring an

93 optimal specific and sensitive detection of these analytes, e.g. eicosanoids and other oxylipins (16) or

94 peptides (17). Among the large number of LC-high resolution-MS (LC-HRMS) methods which has

95 been described for the analysis of lipids in biological samples such as plasma (8, 11), serum (18) or

96 liver (10), only few characterize and optimize the instrumental parameters including source parameters

97 for ionization efficiency as well as parameter settings for Full MS and data-dependent acquisition. For

98 example, Narváez et al. optimized the MS parameters of the Q Exactive HF for the analysis of

99 phospholipids in rat plasma but provide no information about the effects of the parameters (10).

100 Overall, the main focus of method development/characterization of current lipidomics

101 approaches is set on the bioinformatic processing of the LC-MS data. For example, the performance of

102 extraction procedures (19, 20) and chromatographic separation (8, 11) is usually evaluated based on the

103 number of identified lipid species by the bioinformatic software. However, characterization of

104   ionization efficiency and extraction yield of representative lipid species as it is carried out in targeted

105   LC-MS/MS analysis are limited and only described in few untargeted approaches (21).

106   The aim of this work was developing and optimizing extraction, separation and detection of an

107   untargeted LC-HRMS method for the identification and semi-quantitative analysis of lipids with a focus

108   on phospholipids. The careful optimization of the MS parameters allowed to improve the ionization

109   efficiency of the phospholipids. The optimization of the chromatographic separation on two different

110   columns aimed to achieve a broad elution range for phospholipids allowing to detect more analytes by

111   Full MS/ddMS^2 acquisition. Combined with the ionization in both modes, it enabled to acquire a broader

112   spectrum of lipids and to confirm the characterization of tentatively identified lipids. Semi-

113   quantification of polar lipids was performed using one internal standard per lipid class. Two liquid-

114   liquid extraction protocols were compared and evaluated regarding extraction efficiency of internal

115   standards and intra- and inter-day variability. Matrix effects were investigated by ion suppression

116   analysis using two different pools of plasma, unveiling ion suppression as well as ion enhancement

117   effects. Finally, the method was applied to investigate the effects of n3-polyunsaturated fatty acid

118   (PUFA) supplementation on the human plasma lipidome. Here, we could identify distinct phospholipids

119   which were increased and decreased by 12 months of n3-PUFA supplementation.

120   **Material and Methods**

121   **Chemicals**

122   SPLASH Lipidomix Mass Spec Standard mixture containing deuterium labeled lipids from 14

123   different lipid classes (lysophosphatidylcholine (LPC) 18:1[D7]/0:0, lysophosphatidylethanolamine

124   (LPE)   18:1[D7]/0:0,   monoacylglycerol   (MG)   18:1[D7]/0:0/0:0,   phosphatidylserine   (PS)

125   15:0/18:1[D7], phosphatidylinositol (PI) 15:0/18:1[D7], phosphatidylglycerol (PG) 15:0/18:1[D7],

126   phosphatidic acid (PA) 15:0/18:1[D7], sphingomyelin (SM) 18:1;2O/18:1[D7], phosphatidylcholine

127   (PC)   15:0/18:1[D7],   phosphatidylethanolamine   (PE)   15:0/18:1[D7],   diacylglycerol   (DG)

128   15:0/18:1[D7]/0:0, triacylglycerol (TG) 15:0/18:1[D7]/15:0, cholesteryl ester (Chol Ester) 18:1[D7]

129   and free cholesterol (FC) [D7]; 550 nM – 5 µM; concentrations relative to ratios in human plasma, for

130   individual concentrations of the standards in the plasma extract see Table 1) and phospholipid standards

131 PC 16:0/20:4(5Z,8Z,11Z,14Z), PE 18:1(9Z)/18:1(9Z) and PE 14:0/14:0 were purchased from Avanti

132 Polar Lipids (local supplier: Merck KGaA, Darmstadt). PC 18:2(9Z,12Z)/18:2(9Z,12Z), PC

133 18:0/20:5(5Z,8Z,11Z,14Z,17Z), PC 18:0/22:6(4Z,7Z,10Z,13Z,16Z,19Z), PE

134 18:0/20:4(5Z,8Z,11Z,14Z) and PE 18:0/22:4(7Z,10Z,13Z,16Z) used for targeted LC-MS/MS were

135 from Cayman Chemical (local supplier: Biomol, Hamburg, Germany).

136 Acetonitrile (ACN) LC-MS grade, methanol (MeOH) LC-MS grade, *iso*-propanol (IPA) LC-

137 MS grade, chloroform (CHCl$_3$) HPLC grade, formic acid LC-MS grade, as well as *n*-hexane HPLC

138 grade were obtained from Fisher Scientific (Schwerte, Germany). Ultra-pure water (18.2 MΩ) was

139 generated using the Barnstead Genpure Pro system from Thermo Fisher Scientific (Langenselbold,

140 Germany). Ammonium formate was supplied by Sigma-Aldrich (Schnelldorf, Germany). All other

141 chemicals, including *tert*-butyl methyl ether (MTBE) were purchased from Merck KGaA (Darmstadt,

142 Germany).

143 For method characterization, 3 different pools of human plasma were generated. The blood was

144 collected from healthy human subjects in accordance with the guidelines of the Declaration of Helsinki

145 and approved by the ethics committee of the University of Wuppertal. The blood was collected in EDTA

146 tubes and centrifuged (4 °C, 10 min, 1200 x *g*). The plasma was collected, aliquoted and stored at -

147 80 °C as described in (22).

148 **Lipid extraction**

149 *Extraction using MeOH and MTBE.* Lipids in plasma were extracted using a modified liquid-

150 liquid extraction (LLE) based on Matyash et al. (23, 24). Briefly, 10 µL freshly thawed plasma were

151 transferred to glass tubes followed by the addition of 10 µL SPLASH internal standards (IS). 225 µL

152 MeOH were added and samples were vortexed shortly. Then, 750 µL MTBE were added and samples

153 were thoroughly vortexed for 2 min. Phase separation was induced by addition of 188 µL 150 mM

154 ammonium acetate and centrifugation (4 °C, 10 min, 1000 x *g*). The upper organic phase was carefully

155 collected in glass tubes containing 6 µL 30% glycerol in MeOH and the lower phase was re-extracted

156 by addition of 300 µL MTBE. The samples were vortexed for 1 min and centrifuged again (4 °C, 5 min,

157 1000 x *g*). The combined upper phases were evaporated to dryness using a vacuum concentrator

158   (1 mbar, 30 °C, ∼70 min; Christ, Osterode am Harz, Germany). The residue was reconstituted in 50 μL

159   of 50/50 mobile phase (A/B, *v/v* without modifier, i.e. IPA/ACN/H_2O (45/35/20, *v/v/v*)) containing

160   200 nM PE 14:0/14:0 as IS2. Samples were sonicated, centrifuged and transferred to vials for LC-

161   HRMS analysis.

162   *Extraction using IPA, n-hexane, CHCl₃ and MeOH (25).* Lipids in plasma were extracted using

163   a two-stepped LLE (26, 27). 10 μL freshly thawed plasma were transferred to glass tubes followed by

164   the addition of 10 μL IS (SPLASH) and 185 μL water. After addition of 1 μL glacial acetic acid, the

165   phase separation was induced with 500 μL 1 M acetic acid/IPA/*n*-hexane (2/20/30, *v/v/v*) and samples

166   were vortexed for 1 min. 500 μL *n*-hexane were then added, samples were vortexed again for 1 min and

167   centrifuged (room temperature, 10 min, 1000 x *g*). The upper phase was carefully collected in glass

168   tubes containing 6 μL 30% glycerol in MeOH. The lower phase was washed with 500 μL *n*-hexane,

169   vortexed for 1 min, centrifuged again (room temperature, 10 min, 1000 x *g*) and the upper layers were

170   combined. In the second step of the extraction, 750 μL CHCl₃/MeOH (1/2, *v/v*) were added to the lower

171   aqueous phase and samples were vortexed for 1 min. 250 μL CHCl₃ were further added and samples

172   were vortexed again for 1 min. Phase separation was induced by addition of 250 μL 150 mM

173   ammonium acetate and centrifugation (room temperature, 10 min, 1000 x *g*). The upper phase was

174   discarded and the lower phase was collected and combined with the upper phases from the first

175   extraction step. The combined organic phases containing the lipids of both extraction steps were

176   evaporated to dryness using a vacuum concentrator (1 mbar, 30 °C, ∼70 min). The residue was

177   reconstituted in 50 μL IPA/ACN/H_2O (45/35/20, *v/v/v*) containing 200 nM PE 14:0/14:0 as IS2,

178   sonicated, centrifuged and transferred to vials for LC-HRMS analysis.

Method characterization

180   Two established LLE protocols used in the lipidomics field were tested and compared regarding

181   their extraction recovery of major lipid classes from plasma: a protocol using MeOH/MTBE based on

182   a modified procedure according to Matyash et al. (23), and a two-stepped extraction using acetic

183   acid/IPA/*n*-hexane based on Hara et al. (27) for the first step and CHCl₃/MeOH based on Bligh and

184   Dyer (26) for the second (25).

185   Extraction efficiency was evaluated for both protocols on three different days by determining

186   the recovery of the IS spiked to the sample prior to extraction normalized to the IS2 (i.e. PE 14:0/14:0),

187   which was added in the last step before LC-HRMS analysis. The recovery was calculated relative to the

188   recovery of an IS solution directly injected.

189   Further lipid extraction was carried out using MeOH/MTBE. Robustness of extraction was

190   assessed by three different operators on three different days using three different pools of plasma.

191   Effects of matrix were investigated by assessing the extraction recovery of IS added to plasma prior or

192   post extraction and also using different volumes of plasma for extraction. Furthermore, matrix effects

193   were determined by ion suppression analysis by postcolumnly infusing a diluted (0.37-10 µM)

194   SPLASH solution (5 µL/min) mixed *via* a T-piece with the LC-flow (260 µL/min) after injection of a

195   plasma extract without IS (Fig. 3-4).

196   **Untargeted LC-HRMS instrument method**

197   Untargeted lipidomics analysis was performed on a Vanquish Horizon ultra-high-performance

198   liquid chromatography system composed of an autosampler, a binary pump and a column oven coupled

199   to a hybrid quadrupole-orbitrap mass spectrometer (Q Exactive HF) (Thermo Fisher Scientific,

200   Dreieich, Germany). Samples (5 µL) were injected into the LC-HRMS system using an autosampler

201   equipped with a 25 µL sample loop. The sample rack was kept at 10 °C. Two columns were tested for

202   the separation, i.e. ZORBAX Eclipse Plus RRHT C18 (2.1 x 150 mm, 1.8 µm, 95 Å; Agilent,

203   Waldbronn, Germany) and ACQUITY Premier CSH C18 (2.1 x 100 mm, 1.7 µm, 130 Å; Waters,

204   Eschborn, Germany). A binary gradient was used with eluent A (H$_2$O/ACN, 40/60, *v/v*) and eluent B

205   (IPA/ACN, 90/10, *v/v*, 1% H$_2$O), both containing 10 mM ammonium formate and 0.1% formic acid.

206   The optimized chromatographic separation was carried out on the ACQUITY Premier CSH C18 column

207   equipped with a guard column (2.1 x 5 mm, 1.7 µm) at 40 °C using the following gradient with a flow

208   rate of 260 µL/min: 0–0.7 min 30% B; 0.7–0.8 min 30–52.5% B; 0.8–11 min 52.5% B; 11–20 min

209   52.5–60% B; 20–22 min 60–99% B; 22–26 min 99% B; 26–28 min 30% B for column washing and re-

210   equilibration. The total analysis time was 28 min.

211   Lipids were analyzed following positive and negative electrospray ionization in two separate

212   runs using a heated electrospray ionization (HESI) source. For optimization of ionization parameters

213   PC 16:0/20:4(5Z,8Z,11Z,14Z) and PE 18:1(9Z)/18:1(9Z) were chosen as representative lipids for two

214   abundant phospholipid classes found in plasma. Optimization was done in positive and negative mode

215   by infusion of the standards (each 300 nM) (Fig. 1) *via* a syringe pump with 5 µL/min combined *via* a

216   T-piece with an LC-flow of 260 µL/min at an eluent composition of 70% B. Alternatively, also flow

217   injection analysis injecting 5 µL of the standards in the LCflow (i.e., 260 µL/min) was used. Optimized

218   settings are summarized in Fig. 1. These standards were also used for the optimization of the normalized

219   collision energy (NCE) (Fig. S2).

220   As sheath gas, auxiliary gas, sweep gas, as well as collision gas nitrogen was used, generated

221   from compressed air further purified with the purifier RAMS05Z, and combined with the NGM33

222   nitrogen generator (CMC instruments, Eschborn, Germany). The offset of the sprayer was side-to-side

223   +1, front-to-back 1.75 µm, and depth between C- and D-ring.

224   MS detection was carried out in Full MS data-dependent (dd) MS^2 TOP N mode (Full

225   MS/ddMS^2). For Full MS scans, data were acquired over a mass range of *m/z* 200-1200, for both

226   positive and negative ionization modes. The Full MS scans were recorded at a resolution setting of

227   60,000 with the automatic gain control (AGC) target set to 1×10^6 and a maximum ion injection time

228   (IT) of 160 ms. Data-dependent scans from the TOP N *m/z* detected in the Full MS scans were triggered

229   based on an exclusion and inclusion list specific for positive and negative ionization (Table S1 and S2)

230   and a minimum AGC target of 2×10^3 considering an apex trigger of $1 - 4$ s and a dynamic exclusion

231   time of 4 s. MS^2 scans were acquired from the triggered *m/z* with an isolation window of *m/z* 1.5 using

232   NCE combining 20 and 25 relative to *m/z* 500, at a resolution setting of 15,000 with an AGC target of

233   5×10^4 and a maximum IT of 80 ms. In order to ensure enough data points across the chromatographic

234   peaks in Full MS mode for semi-quantitative evaluation, the analysis time was split into segments with

235   different numbers of MS^2 scans triggered during one duty cycle: between 0-7 min TOP 5, between 7-

236   12 min TOP 10 and between 12-28 min TOP 15.

237   Mass accuracy was assured using the following lock masses at the beginning of the run: in

238   positive mode *m/z* 391.2843 (polytetrafluoroethylene) between 1.1-1.2 min and in negative mode

239 *m/z* 265.1479 (sodium dodecyl sulfate) between 1.55-1.65 min. Mass calibration was carried out every

240 72 hours by infusion of Pierce LTQ Velos ESI Positive Ion Calibration Solution and Pierce ESI

241 Negative Ion Calibration Solution (Thermo Fisher Scientific, Langenselbold, Germany).

242   For data acquisition and instrument control Chromeleon software (version 7.2.11, Thermo

243 Fisher Scientific) was used.

244

245 **Targeted LC-MS/MS instrument method**

246 Targeted LC-MS/MS analysis of selected phospholipids was carried out using a 1290 Infinity II

247 (Agilent, Waldbronn, Germany) LC system composed of an autosampler, a binary pump and a column

248 oven. The separation of the lipids was achieved using the same chromatographic conditions described

249 for the untargeted LC-HRMS method. The LC system was coupled to a QTRAP 6500+ mass

250 spectrometer (Sciex, Darmstadt, Germany) operated in negative electrospray ionization mode with the

251 following settings: ion spray voltage -4500 V, source temperature 650 °C, nebulizer gas (GS1,

252 compressed air purified with RAMS05Z; CMC instruments, Eschborn, Germany) 60 psi and drying gas

253 (GS2, purified compressed air) 60 psi, curtain gas (nitrogen, generated with the nitrogen generator Eco

254 Inert-ESP4; DWT, Bottrop, Germany) 35 psi, collision gas (nitrogen) 6 psi. MS detection was carried

255 out in scheduled multiple reaction monitoring (MRM) mode acquiring two transitions per phospholipid:

256 one for quantification and one for qualification resulting from the cleavage of the individual fatty acyl

257 chains. The detection window was set to 180 s around the retention time and the cycle time to 0.4 s.

258 Declustering potentials (DP), entrance potentials (EP), collision cell exit potentials (CXP) and collision

259 energies (CE) were optimized for each of the phospholipids using flow injection analysis with standards

260 (Fig. S7). MS parameters for targeted phospholipid analysis can be found in Table S4. Analyst (Sciex,

261 version 1.7) was used for instrument control and data acquisition, and Multiquant (Sciex, version 2.1.1)

262 for data evaluation.

263   For calibration, stock solutions of the individual phospholipids PC 18:2(9Z,12Z)/18:2(9Z,12Z),

264 PC   18:0/20:5(5Z,8Z,11Z,14Z,17Z),   PC   18:0/22:6(4Z,7Z,10Z,13Z,16Z,19Z),   PE

265 18:0/20:4(5Z,8Z,11Z,14Z) and PE 18:0/22:4(7Z,10Z,13Z,16Z) were mixed and diluted in glass

266 volumetric flasks (5 mL) with ACN/IPA (50/50, *v/v*) at 9 concentration levels. Each calibration level

267   contained the same amount of the IS (SPLASH) comprising one labeled phospholipid from each lipid

268   class (400 nM for PC 15:0/18:1[D7] and 15 nM for PE 15:0/18:1[D7]). Calibration curves were

269   calculated using linear least square regression (weighting: $1/x^2$). Analyte quantification was carried out

270   based on the analyte to corresponding IS peak area ratio using the obtained calibration curves. Linearity

271   was assessed using standard solutions covering a concentration range from 0.2 to 1000 nM. The limit

272   of detection (LOD) was determined as the concentration yielding a signal-to-noise ratio (S/N, peak to

273   peak) ≥3. The concentration with a S/N ≥5 and an accuracy of 80–120% within the calibration curve

274   was defined as lower limit of quantification (LLOQ) and set as the lowest concentration of the

275   calibration curve (Table S4).

276 n3-PUFA supplementation study

277   The effects of n3-PUFA supplementation on the lipid pattern were investigated in plasma

278   samples derived from a double-blinded, randomized, controlled intervention trial (28). A subset of

279   human plasma samples from 20 participants (9 males, 11 females, age 23-72 years) out of 42 subjects

280   who received n3-PUFA capsules containing EPA and DHA corresponding to 4 portions of fatty fish

281   per week (1.5 g EPA and 1.77 g DHA as triacylglycerols per portion) was selected. Criteria for the

282   inclusion/exclusion of subjects are summarized in Figure S8. Plasma samples of the individual

283   participants at baseline (before supplementation) and after 12 months of supplementation were extracted

284   using the LLE with MeOH/MTBE and analyzed by the untargeted LC-HRMS method in randomized

285   order.

286 Data processing

287   Raw data acquired in positive and negative ionization mode by untargeted LC-HRMS analysis

288   were processed using MS-DIAL software (version 4.70) (29) for feature detection, spectra

289   deconvolution and peak alignment between samples. Parameter settings for data processing by MS-

290   DIAL are summarized in Table S3. Each detected feature was manually reviewed and assigned to a

291   putative lipid class and to one of the three different categories (i.e., Confidence, Unsettled or Unknown)

292   based on its retention time and fragmentation spectrum according to following criteria: lipid class

293   assignment was done based on following plausible retention times: lysophospholipids (≤8 min),

294   glycerophospholipids (≥4 min), SM (≥4 min), DG (≥12 min) and TG (≥15 min). Features assigned to

295   one of the mentioned lipid classes with a retention time outside the defined range were flagged as

296   "Unknown" and were not further evaluated. An "Unsettled" feature with an identification score between

297   70 and 75% was flagged as "Confidence" if its fragmentation spectrum contains in positive mode i) the

298   precursor ion, ii) the fragment of a neutral loss of a fatty acyl (e.g. ketene) and iii) characteristic

299   fragments of the lipid class (e.g. *m/z* 184.0733 for PC) (30). In negative mode, a feature was assigned

300   to "Confidence" if its fragmentation spectrum contains i) the fragment of the fatty acyl(s), ii) the

301   fragment of the neutral loss of a fatty acyl (e.g. ketene) and iii) characteristic fragments of the lipid class

302   (e.g. *m/z* 168.0426 for PC) (30). In case one of the criteria mentioned above was not fulfilled, the feature

303   remained assigned "Unsettled". Likewise, features having an identification score between 67 and 70%

304   were rated as "Unsettled". All features assigned to "Confidence" and "Unsettled" were included in the

305   further data evaluation. For additional confidence of lipid identification, the retention time of a logical

306   series of lipid species from the same lipid class was plotted against the sum of the fatty acyl chain length

307   or the sum of the number of double bonds according to Vankova et al. (12) (Fig. S9-10).

308   The peak heights of features detected in positive and/or negative mode derived from MS-DIAL

309   data evaluation were normalized to peak heights of the IS from the same lipid class. For the individual

310   features fold changes between baseline (before supplementation) and after 12 months of

311   supplementation were calculated for individual participants. Using t-test, for the individual features *p*-

312   values for the mean of the normalized peak height changes before and after supplementation were

313   determined. Volcano plots were created by plotting the mean of log2 (fold change) against the -log10

314   (*p*-value).

315   Putatively identified phospholipids which changed most after n3-PUFA supplementation and

316   were commercially available, were quantified by targeted LC-MS/MS using the same plasma extracts

317   diluted 1:50 in ACN/IPA (50/50, *v/v*).

318   **Lipid notation**

319   The shorthand notation of the lipids is based on Liebisch et al. using the separator "_" if the *sn*-position

320   of the fatty acyl(s) chain is unknown, while the separator "/" indicates a proven *sn*-position (with *sn*-

321   1/*sn*-2) (31). The position of the double bonds, e.g. PC 16:0/20:4(5Z,8Z,11Z,14Z), was specified only

322   if confirmed by authentic standards.

Results and discussion

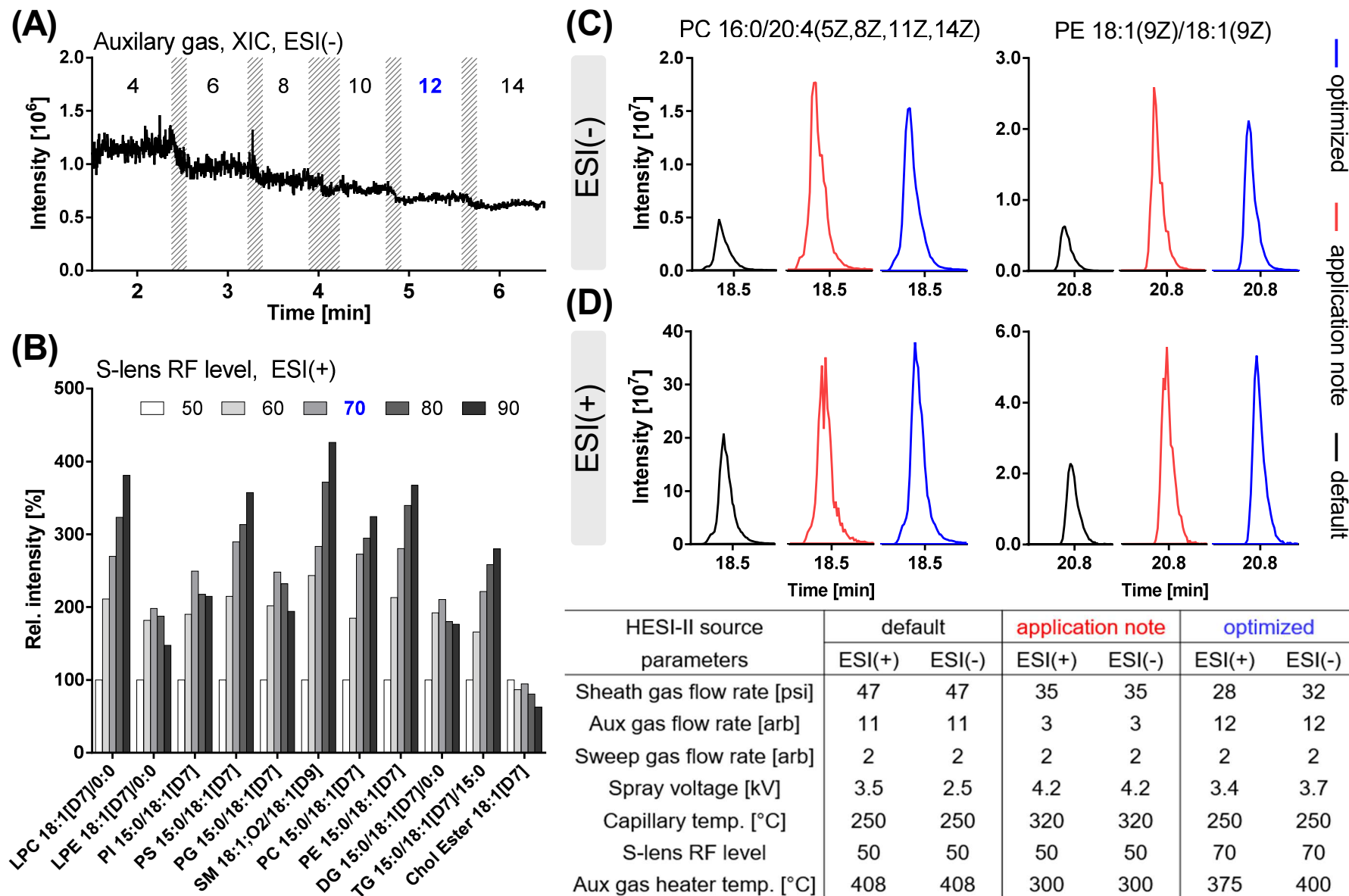### Optimization of mass spectrometric parameters

325   Sensitive as well as selective mass spectrometric analysis of phospholipids in biological

326   samples requires careful optimization of instrument parameters. Mass spectrometric detection of

327   phospholipids is feasible after positive (ESI(+)) and negative (ESI(-)) ionization due to their polar head

328   group by forming different types of adducts (6), while DG, TG and Chol Ester can only be efficiently

329   ionized in positive mode (8, 32). Analysis of lipids was carried out in positive and negative mode in

330   two separate runs to enable characterization of the lipid class as well as the fatty acyl chains based on

331   characteristic fragmentation behavior. The instrument software sets default settings for the source

332   parameters based on the LC flow rate. Starting from these settings, the source parameters of the HESI

333   source (i.e. spray voltage, sheath gas, auxiliary gas, auxiliary gas heater temperature, sweep gas,

334   capillary temperature) and the S-lens RF level were optimized in both ionization modes, and compared

335   with the default settings and the settings described in an application note for lipidomics analysis with

336   the same flow rate (260 µL/min) from the instrument manufacturer (33). The optimization of the spray

337   voltage, the sheath gas, the sweep gas and the capillary temperature showed only minor impact on the

338   signal intensity, and is described in detail in the supplementary information (Fig. S1).

339

340

341

342

343

HESI-II source parameters	default		application note		optimized	
	ESI(+)	ESI(−)	ESI(+)	ESI(−)	ESI(+)	ESI(−)
Sheath gas flow rate [psi]	47	47	35	35	28	32
Aux gas flow rate [arb]	11	11	3	3	12	12
Sweep gas flow rate [arb]	2	2	2	2	2	2
Spray voltage [kV]	3.5	2.5	4.2	4.2	3.4	3.7
Capillary temp. [°C]	250	250	320	320	250	250
S-lens RF level	50	50	50	50	70	70
Aux gas heater temp. [°C]	408	408	300	300	375	400

Fig. 1: Effect of selected ion source parameters on intensity and stability of the ESI-MS signal. Shown is **(A)** the influence of the auxiliary gas flow rate on the signal in ESI(-) mode during infusion of a phospholipid standard containing PC 16:0/20:4(5Z,8Z,11Z,14Z) and PE 18:1(9Z)/18:1(9Z) while other parameters were set to default; **(B)** the effect of the S-lens RF-level on signal intensity relative to a value of 50 for different deuterium-labeled lipids; **(C and D)** peak intensity and shape of PC 16:0/20:4(5Z,8Z,11Z,14Z) and PE 18:1(9Z)/18:1(9Z) in *(TOP, C)* ESI(-) and *(BOTTOM, D)* ESI(+) mode using default parameters, parameters of an application note for lipidomics from the manufacturer [33], or parameters after optimization.

344   The heated auxiliary gas flow was optimized in combination with the auxiliary gas heater

345   temperature and showed the greatest impact among all source parameters on spray stability in both

346   ionization modes. It was optimized in a range of 4 – 14 arbitrary units (Fig. 1A). A value of 4 resulted

347   in a noisy and unstable spray, and increasing the auxiliary gas flow decreased the noise but also

348   decreased the signal intensity. A value of 12 was selected for both ionization modes in order to minimize

349   the noise of the spray without losing too much sensitivity. The value selected for the auxiliary gas flow

350   is close to the default settings (i.e. 11), but clearly higher than the value used in the application note

351   (i.e. 3) (33). However, the peak shape of the phospholipids is clearly improved when a higher value is

352   used (Fig. 1C-D). Our results are in line with previous studies employing with the same instrument an

353   auxiliary gas flow of 10 for the analysis of phospholipids in serum at an LC flow rate of 400 µL/min

354   (34), or in pituitary adenoma tissues at an LC flow rate of 260 µL/min (7); or an auxiliary gas flow of

355   15 for the analysis of human plasma lipids at an LC flow rate of 325 µL/min (11).

356   Transfer of ions from the ion transfer tube to the ion optics through the S-lens is achieved by

357   the RF amplitude applied to the electrodes of the S-lens. The S-lens RF level is a numerical factor

358   affecting transmission, i.e. a higher S-lens RF level increases transmission of ions with higher m/z while

359   also fragmentation of fragile ions in the S-lens occurs. Optimization of the S-lens RF level was

360   performed using deuterium-labeled lipids (SPLASH) from different lipid classes. Increasing the S-lens

361   RF level from the default value, i.e. 50, increased the ion transmission of all IS except Chol Ester

362   18:1[D7]. For a S-lens RF level of 80 and 90 a decrease in the signal of LPE 18:1[D7], PI 15:0/18:1[D7],

363   PG 15:0/18:1[D7], DG 15:0/18:1[D7]/0:0 was observed. Thus, a S-lens RF level of 70 for both

364   ionization modes was chosen which massively improved the ion transmission of the phospholipids (Fig.

365   1B). The default S-lens RF level of 50 is used in several lipidomic methods using a Q Exactive HF

366   instrument (7, 9, 35). However, our results show that optimization of this parameter has a great impact

367   on the ion transmission and signal intensity and thus should be carefully optimized.

368   Overall, the optimization of the source parameters minimized the noise resulting in a better

369   peak shape, and increased the sensitivity by a factor of 3 in ESI(+) and ESI(-) compared to the default

370   parameters.

Optimization of chromatographic separation

371

372   Liquid chromatographic separation of lipids covering the range from polar lipids such as

373 lysophospholipids to the very hydrophobic ones, e.g. neutral lipids, can be performed using RPLC (5,

374 8, 34, 36). We aimed to optimize the chromatographic conditions in order to achieve an efficient

375 separation between different lipid species with a focus on phospholipids. Since numerous isobaric lipid

376 species, i.e. with the same *m/z* are present in biological samples, liquid chromatographic separation is

377 crucial for their characterization. An isocratic step was included in the gradient to extend the elution

378 window for phospholipids thereby enabling the acquisition of more MS^2 spectra for their

379 characterization in Full MS/ddMS^2 mode.

380   For the liquid chromatographic optimization, we selected three critical pairs of isobaric

381 phospholipids: PC 18:2_20:4/PC 18:1_20:5, PC 18:1_18:2/PC 16:0_20:3 and PC 18:0_18:2/PC

382 18:1_18:1. These are highly abundant in human plasma and have different retention times between 10

383 and 20 min under the applied RPLC conditions. Two RP C18-columns with fully porous sub 2 µm

384 particles for high separation efficiency and sample loading capacity were tested using a lipid extract

385 from human plasma. We chose two columns which were previously successfully used in lipidomics

386 applications, i.e. the ZORBAX Eclipse Plus RRHT C18 (37, 38) and the ACQUITY Premier CSH C18

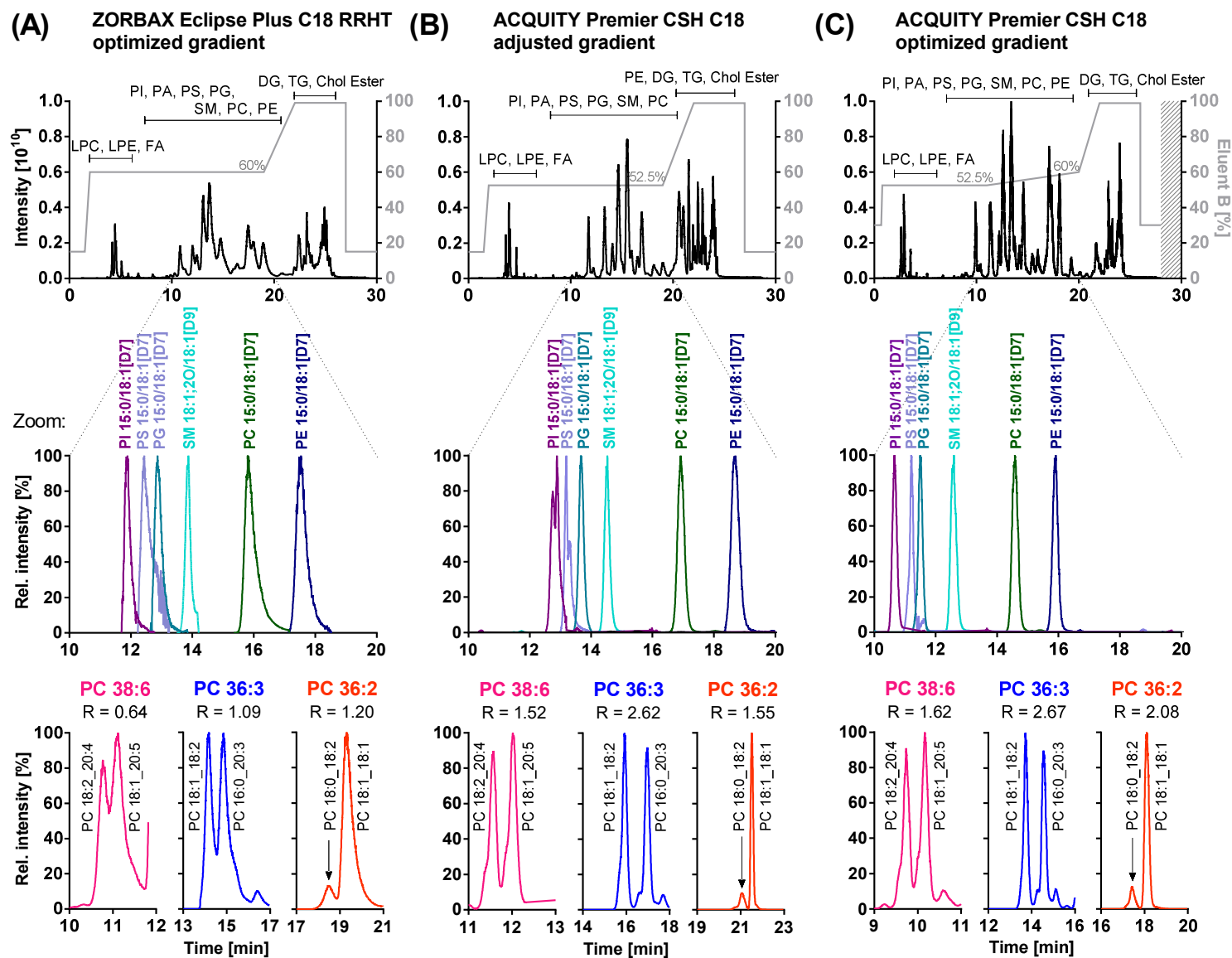387 column (7, 9, 34, 38, 39).

388

389

390

391

392

393

394

395

396

397

Fig. 2: Chromatographic separation efficiency of lipids. Shown is the separation (**TOP**) of a lipid extract from human plasma (Full MS scan *m/z* 200-1200), (**MIDDLE**) of deuterium-labeled IS (respective XIC), and (**BOTTOM**) of isobaric phospholipid species PC 38:6 (*m/z* 806.5694), PC 36:3 (*m/z* 784.5851) and PC 36:2 (*m/z* 786.6007) acquired in ESI(+) mode using (**A**) an optimized gradient on a ZORBAX Eclipse Plus RRHT C18 column (2.1 x 150 mm, 1.8 µm, 95 Å), (**B**) an ACQUITY Premier CSH C18 column (2.1 x 100 mm, 1.7 µm, 130 Å) and a gradient with adjusted elution power and (**C**) an optimized gradient on the latter column. Mobile phases for all separations were eluent A (H$_2$O/ACN (40/60, *v/v*)) and eluent B (IPA/ACN (90/10, *v/v*), 1% H$_2$O), both containing 10 mM ammonium formate and 0.1% formic acid. The fatty acyl chains of the isobaric phospholipids (**BOTTOM**) were characterized based on the fragmentation spectra acquired in ESI(-) mode.

399   Using the ZORBAX Eclipse Plus RRHT C18 column (2.1 x 150 mm, 1.8 µm, 95 Å) with an

400   optimized gradient, lipids from a human plasma extract eluted as relatively broad peaks with a full width

401   at half maximum (FWHM) for the labeled IS PS 15:0/18:1[D7], PC 15:0/18:1[D7] and PE

402   15:0/18:1[D7] of 17.4 s, 19.8 s and 18.9 s, respectively. Phospholipids showed also an asymmetric peak

403   shape with a tailing factor for the labeled phospholipids between 1.62 and 4.38. Overall, this mediocre

404   separation of the lipids is reflected by incomplete separation of the selected critical pairs, i.e. PC

405   18:2_20:4/PC 18:1_20:5 or PC 18:1_18:2/PC 16:0_20:3 with a resolution of 0.64 and 1.09,

406   respectively. Additionally, the pair PC 18:0_18:2/PC 18:1_18:1 was not fully separated (R=1.20) (Fig.

407   2A).

408   The separation on the ACQUITY Premier CSH C18 column (2.1 x 100 mm, 1.7 µm, 130 Å)

409   was carried out with adjusted elution power of the gradient during the isocratic step by lowering the

410   percentage of eluent B from 60 to 52.5% (Fig. 2B). With this column the same elution order was

411   observed, however, the peak shape of the lipids was considerably improved showing narrower peaks

412   and better peak symmetry. No peak tailing was observed for the phospholipids, except for the acidic PS

413   15:0/18:1[D7] (i.e. tailing factor 1.81) (Fig. 2B, middle), which is known in RPLC even when a high

414   aqueous percentage is used for the initial conditions (40). The better performance of this column might

415   be explained by the charged surface of its particles improving peak symmetry with low ionic-strength

416   mobile phases.

417   Separation of phospholipids was also considerably improved with a resolution ≥1.5 for the

418   selected critical pairs, e.g. PC 18:2_20:4/PC 18:1_20:5 (R=1.52) (Fig. 2B, bottom). Nevertheless, using

419   this gradient (Fig. 2B) late eluting PC and PE species still showed broad peaks, e.g. PE 15:0/18:1[D7]

420   eluting at the end of the isocratic step with a FWHM of 16.8 s. Also, more hydrophobic phospholipids

421   eluting after the isocratic step, e.g. PE 18:0_20:4 at 21.7 min or PC 18:0_20:3 at 21.9 min, co-eluted

422   with other late eluting phospholipids as indicated in the TIC (Fig. 2B, top). Thus, the gradient was

423   further optimized by including a shallow linear increase to 60% B after the isocratic step and adjusting

424   the initial percentage of B as well as the time for the final elution and re-equilibration step: The more

425   hydrophobic phospholipids eluted earlier, e.g. PE 18:0_20:4 at 18.6 min and PC 18:0_20:3 at 19.7 min,

426   and their separation was improved. For the starting conditions 30% B was used as isocratic pre-

427 concentration step to focus the analytes at the beginning of the column. With a capacity factor k>1, the

428 retention of the polar LPC 18:1[D7]/0:0 (k=2.71) was sufficient.

429   Overall, with this optimized gradient the peak shape was further improved yielding FWHM for

430 all labeled phospholipids between 10 and 13 s, also for PE 15:0/18:1[D7] (Table 1). Moreover,

431 separation of the critical pairs was optimal with a resolution ≥1.5, i.e.PC 18:2_20:4/PC 18:1_20:5

432 (R=1.62), PC 18:1_18:2/PC 16:0_20:3 (R=2.67) and PC 18:0_18:2/PC 18:1_18:1 (R= 2.08) (Fig. 2C,

433 bottom). The isocratic step at 99% B at the end of the gradient was held for 4 min, which was sufficient

434 to elute the neutral lipids, i.e. TG, DG, Chol Ester (leading to minimal carryover for TG 18:1_18:1_18:1

435 to the next injection (<1%)). Only 2 min re-equilibration were required, resulting in stable retention

436 times for the lysophospholipids in the following injection. Including re-equilibration, the final run time

437 of the optimized method was 28 min covering polar as well as neutral lipids and the method showed

438 stable retention times with an intra-batch (n=92) relative standard deviation (RSD) <0.71% (0.08 min)

439 (Table 1).

440

441

442

443

444

445

446

447

448

449

450

451

452

Table 1: Characterization of mass spectrometric and chromatographic parameters of deuterium-labeled lipids used as IS. Shown are the molecular formula, the mass-to-charge ratio (*m/z*) of the most intense adduct measured in ESI(+) and ESI(-) mode, the concentration of the IS in the plasma extract, the retention time (t_R) and the full width at half maximum (FWHM) of the chromatographic peak using the LC-HRMS method.

analyte	molecular formula	ESI(-)		ESI(+)		concentration [μM]	$t_R \pm SD$ [min] (rel. SD)[1]	FWHM[1] $\pm$ SD [s]
		m/z	adduct type	*m/z*	adduct type			
LPC 18:1[D7]/0:0	$C_{26}H_{45}D_7NO_7P$	573.3903	[M+COOH]$^-$	529.3994	[M+H]$^+$	4.5	2.88 ± 0.01 (0.31%)	3.98 ± 0.46
LPE 18:1[D7]/0:0	$C_{23}H_{39}D_7NO_7P$	485.3379	[M-H]$^-$	487.3524	[M+H]$^+$	1.0	2.97 ± 0.01 (0.32%)	4.15 ± 0.65
PI 15:0/18:1[D7]	$C_{42}H_{75}D_7NO_{13}P$	828.5625	[M-H]$^-$	847.6036	[M+H]$^+$	1.0	10.58 ± 0.04 (0.38%)	10.04 ± 0.48
PS 15:0/18:1[D7]	$C_{39}H_{67}D_7NO_{10}P$	753.5417	[M-H]$^-$	755.5562	[M+H]$^+$	0.50	11.13 ± 0.08 (0.71%)	12.55 ± 1.02
PG 15:0/18:1[D7]	$C_{39}H_{68}D_7O_{10}P$	740.5464	[M-H]$^-$	759.5875	[M+NH$_4$]$^+$	3.5	11.43 ± 0.05 (0.42%)	10.75 ± 1.19
SM 18:1;2O/18:1[D9]	$C_{41}H_{72}D_9N_2O_6P$	782.6379	[M+COOH]$^-$	738.6470	[M+H]$^+$	4.0	12.77 ± 0.05 (0.38%)	11.92 ± 1.00
PC 15:0/18:1[D7]	$C_{41}H_{73}D_7NO_8P$	797.6049	[M+COOH]$^-$	753.6134	[M+H]$^+$	20	14.89 ± 0.05 (0.35%)	12.25 ± 1.5
PE 15:0/18:1[D7]	$C_{38}H_{67}D_7NO_8P$	709.5519	[M-H]$^-$	711.5664	[M+H]$^+$	0.75	16.17 ± 0.05 (0.33%)	12.33 ± 0.39
DG 15:0/18:1[D7]/0:0	$C_{36}H_{61}D_7O_5$	[2]	-	605.5844	[M+NH$_4$]$^+$	1.5	22.42 ± 0.02 (0.08%)	3.98 ± 0.53
TG 15:0/18:1[D7]/15:0	$C_{51}H_{89}D_7O_6$	[2]	-	829.7985	[M+NH$_4$]$^+$	6.5	23.97 ± 0.01 (0.03%)	3.60 ± 0.36
Chol Ester 18:1[D7]	$C_{45}H_{71}D_7O_2$	[2]	-	675.6779	[M+NH$_4$]$^+$	50	24.35 ± 0.01 (0.04%)	3.87 ± 0.47

[1]t_R and FWHM were determined as mean in plasma extracts which were pre-spiked with IS mixture and measured on 6 different days (n=92)

[2]DG 15:0/18:1[D7]/0:0, TG 15:0/18:1[D7]/0:0, Chol Ester 18:1[D7] are only detected in ESI(+) mode

Optimization of parameters for Full MS/data-dependent MS^2 (TOP N) acquisition

Acquisition of data in Full MS/ddMS^2 TOP N mode allows in addition to the determination of the exact mass of the detected lipid species by HRMS their characterization based on characteristic product ion spectra. In this mode one full scan (the survey scan) is recorded, followed by the acquisition of a distinct number (N) of product ion spectra of selected precursor ions. For reliable analysis of lipids using data-dependent acquisition it is important to balance between: i) acquisition of as many product ion spectra as possible to characterize as many precursor ions as possible and ii) an appropriate cycle time (frequency) enabling to gain enough data points (12 to 20) for the semi-quantification in Full MS mode.

Table 2: Data points across the peaks using Full MS/data-dependent MS^2 (TOP N) acquisition.
Shown are the numbers of MS scans across the full chromatographic peak width using different numbers of data-dependent triggered fragment spectra (TOP N), and the full width at half maximum (FWHM) (mean ± SD, n=4) of selected deuterium-labeled IS. Resolution settings were Full MS: R=60,000; ddMS^2: R=15,000.

	ESI(-)				
analyte	MS scans over the full peak width				FWHM ± SD [s]
	Top 5	Top 10	Top 15	Top 20	
LPC 18:1[D7]/0:0	**13**	7	4	3	2.93 ± 0.13
LPE 18:1[D7]/0:0	**13**	7	5	3	3.17 ± 0.07
PI 15:0/18:1[D7]	32	**17**	12	9	10.6 ± 0.53
PS 15:0/18:1[D7]	34	**17**	11	7	10.5 ± 0.41
PG 15:0/18:1[D7]	34	**15**	11	8	8.03 ± 0.86
SM 18:1;2O/18:1[D9]	44	21	**14**	11	13.2 ± 0.48
PC 15:0/18:1[D7]	44	23	**15**	11	13.4 ± 1.00
PE 15:0/18:1[D7]	41	21	**13**	9	11.7 ± 0.60

The effect of the number of triggered data-dependent MS^2 (TOP N) on the data points across the chromatographic peaks of different labeled lysophospholipids and phospholipids eluting over the chromatographic range was investigated. As expected, with increasing number of the TOP N less data points in Full MS were recorded, and TOP 20 resulted in an insufficiently low number of data points (i.e. 3 to 11 points) per peak (Table 2). For analytes with narrow peaks, e.g. the early eluting lysophospholipids with a FWHM of 3 s only the TOP 5 acquisition led to sufficient data points (i.e. 13 points). However, for later eluting phospholipids this resulted in a high number of data points (>31

482   points) due to their broader peaks (FWHM 10.6 s, Table 2). Thus, a higher TOP N was used for

483   phospholipids yielding more comprehensive qualitative data without forfeiting peak accuracy for

484   quantification. Consequently, the number of ddMS^2 triggered was adjusted in relation to the FWHM

485   determined for the IS taking the cycle time into account using for Full MS R=60,000 and for ddMS^2

486   R=15,000: i.e. 0.8 s for TOP 5 (1 Full MS + 5 ddMS^2), 1.4 s for TOP 10 (1 Full MS + 10 ddMS^2) and

487   2.2 s for TOP 15 (1 Full MS + 15 ddMS^2). For the elution window of the lysophospholipids (i.e.

488   0 – 7 min) TOP 5 was selected, TOP 10 precursor ions were triggered from 7 – 12 min covering

489   phospholipids eluting with a FWHM of 8 – 10 s; and from 12 min until the end of the analysis TOP 15

490   was used covering phospholipids eluting with a FWHM >11 s. As this study focuses on phospholipids,

491   no optimization was done for the late-eluting neutral lipids (i.e. DG, Chol Ester, TG). Because one MS^2

492   spectrum per lipid species, ideally at the apex of the peak, is sufficient for characterization the apex

493   trigger was set from 1 – 4 s and the dynamic exclusion to 4 s allowing on the one hand the acquisition

494   of meaningful spectra at high intensity of the precursor ions and on the other hand the trigger of many

495   different precursor ions. So far, the number of MS^2 scans (TOP N) triggered during one duty cycle was

496   not split into segments over the analysis time in previous studies. Instead, they used constant TOP N

497   ranging from 2, 3, 10 or 20 for the whole analysis time (7-11, 34, 35, 39, 41, 42). Our data shows that

498   the optimization of this parameter is crucial to acquire as many product ion spectra as possible for

499   characterization while keeping sufficient data points for semi-quantification in Full MS. The use of an

500   exclusion list covering common contaminants such as polysiloxanes, alkane polymers or phthalates

501   prevents the acquisition of ddMS^2 of abundant background ions containing no useful information

502   (Table S1). Additionally, using an inclusion list comprising lipids of interest, i.e. PC and PE bearing

503   biologically relevant PUFA (Table S2), ascertains that their ddMS^2 are recorded and thus reliably allows

504   the characterization of their presence in the biological samples.

Optimization of normalized collision energy

506   In order to obtain meaningful product ion spectra enabling comprehensive characterization of

507   the lipid class as well as the fatty acyl chains, we characterized the influence of the collision energy

508   (CE) on MS^2 in both ionization modes (Fig. S2). Lipids present in biological samples cover a wide

509 range of masses. Thus, the NCE was used for fragmentation which represents the CE relative to m/z 500

510 and applies an adjusted actual CE depending on the m/z of the precursor ion, instead of applying the

511 identical absolute CE regardless of the m/z. MS^2 spectra of the selected PC and PE standards were

512 recorded in both ionization modes using a NCE of 10, 20, 25 or 30, and evaluated for characteristic

513 fragments comprising in ESI(+) the fragments of the phospholipids' polar head group or its (partly)

514 loss; and in ESI(-) the fragments resulting from the fatty acyl chains (30).

515   With a NCE of 10 only slight fragmentation was observed: MS^2 spectra were dominated by the

516 molecular ions and only fragments of the polar head group were observed for both phospholipids in

517 both ionization modes (Fig. S2 A-B, top). With a NCE of 20 and 25, the intensity of the fragments

518 related to the polar head group was increased (i.e. m/z 184.0733 for PC, and [M+H-141.0191]$^+$ for PE)

519 in ESI(+). Moreover, in ESI(-) fragments of the fatty acyl chains were detected (Fig. S2 A-B, middle).

520 Further increasing the NCE to 30 decreased the absolute intensity of most characteristic fragments

521 particularly of those with a high m/z.

522   Based on these findings, a stepwise fragmentation of the precursor ions using a combination of

523 NCE 20 and 25 for both ionization modes was applied in the final method. This is in line with previous

524 studies using also a stepwise fragmentation of 20 and 25 in both ionization modes (39), or 20 and 25 in

525 ESI(+) and 20, 24 and 28 in ESI(-) (8).

526 **Sample preparation**

527   Selection of suitable extraction conditions for lipids from biological samples is a key

528 prerequisite in untargeted analysis to ensure coverage of lipids with varying polarity. In the present

529 study, individual lipid species were semi-quantified using one IS per lipid class.

530

531

532

533 **Table 3: Extraction efficiency of IS from human plasma.** Three different pools of human plasma were extracted by LLE on three different days using an
534 one-step MeOH/MTBE extraction or a two-stepped extraction with IPA/n-hexane//CHCl$_3$/MeOH. Shown are the mean values and relative standard deviation
535 (RSD) (n=9 for intra-day, n=27 for inter-day).

536

537

ESI(-)	day 1				day 2				day 3				day 1-3	
	MeOH/MTBE		IPA/n-hexane//CHCl$_3$/MeOH		MeOH/MTBE		IPA/n-hexane//CHCl$_3$/MeOH		MeOH/MTBE		IPA/n-hexane//CHCl$_3$/MeOH		MeOH/MTBE	IPA/n-hexane//CHCl$_3$/MeOH
analyte	recovery [%]	RSD [%]	recovery [%]	RSD [%]	recovery [%]	RSD [%]	recovery [%]	RSD [%]	recovery [%]	RSD [%]	recovery [%]	RSD [%]	RSD$_{interday}$ [%]	RSD$_{interday}$ [%]
LPC 18:1[D7]/0:0	87	3	85	9	82	6	75	8	80	4	76	6	6	10
LPE 18:1[D7]/0:0	90	4	73	8	86	6	78	5	86	5	75	7	5	7
PI 15:0/18:1[D7]	108	5	115	8	105	6	120	5	105	4	108	9	5	9
PS 15:0/18:1[D7]	93	5	4	50	89	9	12	90	91	10	22	57	8	97
PG 15:0/18:1[D7]	88	6	104	8	84	11	87	6	88	19	96	7	13	10
SM 18:1;2O/18:1[D9]	69	9	74	8	70	7	63	10	72	7	68	7	8	11
PC 15:0/18:1[D7]	79	3	93	6	78	5	85	5	82	5	84	7	5	7
PE 15:0/18:1[D7]	82	3	91	3	81	5	94	5	85	5	91	4	5	4

ESI(+)	day 1				day 2				day 3				day 1-3	
	MeOH/MTBE		IPA/n-hexane//CHCl$_3$/MeOH		MeOH/MTBE		IPA/n-hexane//CHCl$_3$/MeOH		MeOH/MTBE		IPA/n-hexane//CHCl$_3$/MeOH		MeOH/MTBE	IPA/n-hexane//CHCl$_3$/MeOH
analyte	recovery [%]	RSD [%]	recovery [%]	RSD [%]	recovery [%]	RSD [%]	recovery [%]	RSD [%]	recovery [%]	RSD [%]	recovery [%]	RSD [%]	RSD$_{interday}$ [%]	RSD$_{interday}$ [%]
LPC 18:1[D7]/0:0	69	5	72	14	67	5	63	6	57	5	55	7	10	15
LPE 18:1[D7]/0:0	89	7	73	7	80	5	71	8	80	4	68	6	7	8
PI 15:0/18:1[D7]	101	7	81	9	96	4	80	6	91	6	80	12	7	9
PS 15:0/18:1[D7]	85	10	3	47	81	13	8	92	78	9	21	61	11	106
PG 15:0/18:1[D7]	65	15	75	11	57	18	76	8	61	15	58	9	16	15
SM 18:1;2O/18:1[D9]	122	7	107	11	115	4	107	6	78	8	84	5	20	14
PC 15:0/18:1[D7]	85	5	94	9	79	3	84	6	73	4	75	4	8	11
PE 15:0/18:1[D7]	126	4	117	9	115	7	129	12	107	9	112	8	10	12

538   Recoveries between the MeOH/MTBE (23) and the two-stepped extraction protocol (25) were

539   comparable for all phospholipid classes covered by the IS except for PS (Table 3). Overall apparent

540   extraction recovery was good being slightly better in ESI(-) with >75% except for SM, while in ESI(+)

541   mode it was >70% except for LPC and PG. Also, reproducibility of the lipid extraction was excellent

542   with an intra-day and inter-day variance <100 ± 15% except for PG and SM (<100 ± 20%). Extraction

543   recovery of PS was considerably lower with the two-stepped extraction (<13% two steps *vs.* >80%

544   MeOH/MTBE) and showed high variation, i.e. intra-day 100 ± 47% and inter-day variance >100 ±

545   97%, in both ionization modes. This poor recovery of PS with the two-stepped extraction is likely due

546   to the addition of acetic acid leading to the protonation of the serine head group and thus the PS

547   (partially) remains in the aqueous phase. With both processing methods also the neutral lipids, i.e. DG,

548   TG and Chol Ester, are extracted. However, if also these more hydrophobic lipids are in the focus of

549   analysis a less polar reconstitution solvent after LLE must be chosen to ensure a better solubilization

550   (32).

551   All in all, the MeOH/MTBE-based LLE is more environmentally friendly (no halogenated

552   solvents) and the collection of the upper phase containing the lipids is easier in comparison to the

553   extraction with $CHCl_3$ where the lipids are in the lower phase. Moreover, it showed better extraction of

554   the PS lipid class. In consequence, the MeOH/MTBE extraction was selected and further characterized.

555   Regarding robustness, the extraction recoveries were not impacted by the plasma pool used for LLE

556   (Fig. S3). Inter-operator variability was thus determined combining all data from three different days

557   and plasmas (n=81), and was excellent (<100 ± 12% in ESI(-) and <100 ± 23% in ESI(+)). Only the

558   extraction of PS was affected by the operator, showing a recovery <56% when samples were prepared

559   by operator 2 while >80% were recovered by operator 1 and 3, which is reflected by an inter-operator

560   variance of 100 ± 33%. Comparison of extraction recoveries of IS spiked to plasma prior or post

561   extraction unveiled that apparent losses of IS during sample preparation are <15% for the

562   lysophospholipids and <8% for phospholipids in both ionization modes (Fig. 3A-B). These losses

563   during sample preparation were slightly better than those reported by a modified Matyash protocol with

564   an average loss of 27% (43). Low apparent recoveries were observed particularly for PG 15:0/18:1[D7]

565   in ESI(+) (50%) when the IS was added after extraction. These losses in the signal thus occur during

566   LC-MS analysis due to ion suppression.

567   **Ion suppression analysis**

568   Ion suppression analysis showed in ESI(+) a strong suppression of the signal of PG

569   15:0/18:1[D7] (approx. 50%) at its elution time, while in ESI(-) the signal was less affected. This

570   confirms the results of the spiking experiments and might explain the higher variance of the recovery

571   of PG (Fig. 3, Table 3, Fig. S3). Overall, ion suppression analysis revealed stronger ion suppression

572   effects in ESI(+) compared to ESI(-), and was similar for the different investigated plasma pools.

573   Besides ion suppression also ion enhancement effects were observed at the corresponding elution times,

574   e.g. for SM 18:1;2O/18:1[D7] and PE 15:0/18:1[D7] in ESI(+), and for PI 15:0/18:1[D7] in ESI(-) (not

575   shown).

576   Extraction of a higher plasma volume (i.e., 20 and 50 µL) increased the ion suppression effects

577   in ESI(+), especially for SM 18:1;O2/18:1[D9]. In ESI(-), besides ion suppression, strong ion

578   enhancement was observed for PI 15:0/18:1[D7] and PG 15:0/18:1[D7] with higher plasma volume

579   (Fig. S4). Thus, the use of 10 µL plasma is preferred as here ion suppression effects of the IS were

580   acceptable. This sample volume is in line with previous lipidomics methods, e.g. Wang et al. and Chen

581   et al. used 10 µL of human plasma for the extraction of lipids using a MeOH/MTBE-based LLE (44,

582   45); and Ottestad et al. extracted lipids from 10 µL of human plasma using a mixture of $CHCl_3$/MeOH
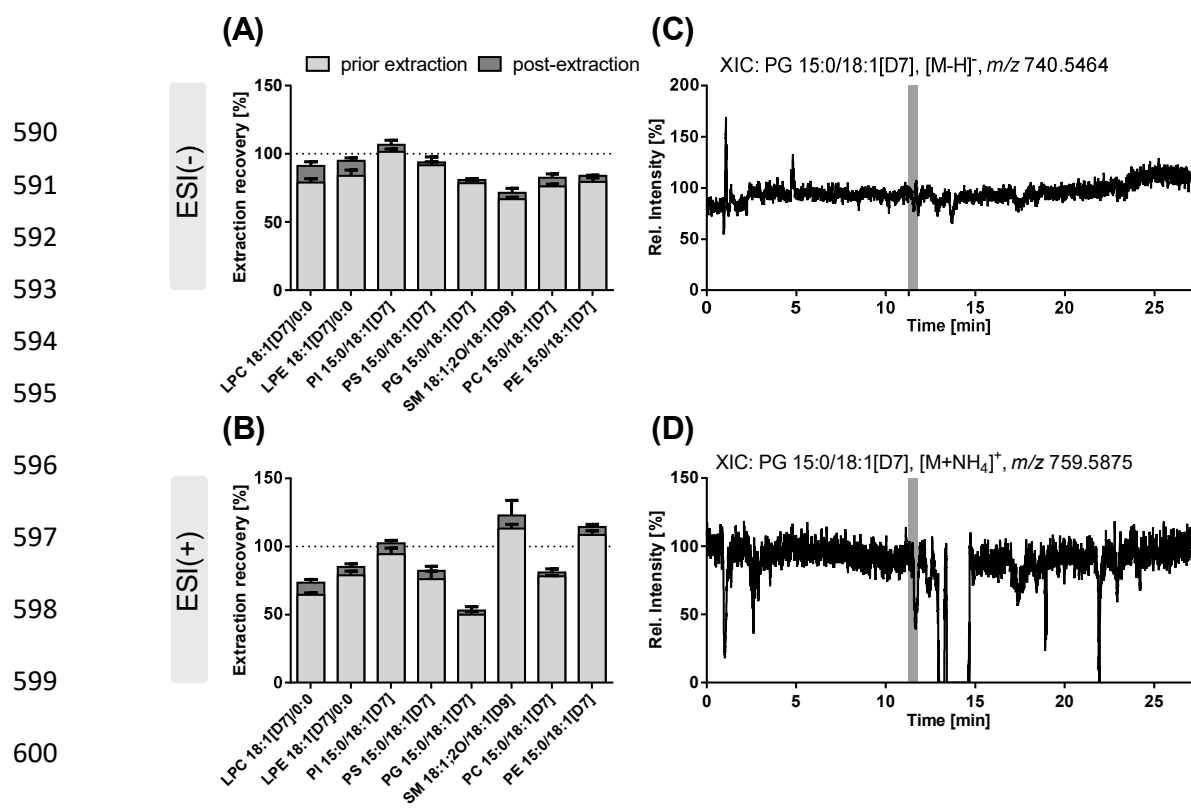
583   (46).

584

585

586

587

588

589

Fig. 3: Influence of ion suppression on the extraction recovery from plasma. Shown are the recoveries of deuterium-labeled IS from the extraction of 10 µL of human plasma **(A)** in ESI(-) and **(B)** in ESI(+) mode. IS were spiked to the plasma at the beginning of sample preparation (prior extraction) or after sample preparation directly before measurement (post extraction). Shown are mean values ± SD, n=3. **(C)** and **(D)**, an IS solution (1.9 µM, 5 µL/min) was post-columnly mixed with the LC-flow (260 µL/min) following injection of a plasma extract. Shown are the XIC of PG 15:0/18:1[D7] in **(C)** ESI(-) and **(D)** ESI(+) mode. The grey bar indicates the retention time of PG 15:0/18:1[D7].

Excursus: Deletion of MS signals by orbitrap MS

Ion suppression analysis unveiled in ESI(+) a complete drop of the signal of PG 15:0/18:1[D7] ([M+NH$_4$]$^+$ m/z 759.5875) to zero on two retention times between 13.24 to 15.17 min (for 116 s) (Fig. 3D and Fig. 4). Increasing the resolution setting of the full scan from 60,000 to 240,000 decreased this signal drop to 32 s but it still occurred even at the highest resolution (Fig. 4A). Full MS spectra indicate a distortion of the m/z by an interfering analyte resulting in a mass deviation >20 ppm for the m/z of PG 15:0/18:1[D7] ([M+NH$_4$]$^+$) at both retention times (Fig. 4B). Based on the m/z determined in the lipid extract without IS infusion, as well as its MS^2 spectra, the interference could be related to the [^{13}C$_1$] isotope of PC 16:0_18:2 ([M+H]$^+$ m/z 759.5728) which is present at high abundance in the plasma lipid extract (Fig. 4C). The elution window of this analyte from 13.30 to 15.01 min fits to the deletion of the signal. The separation of this interfering m/z was achieved at 13.41 min with a resolution of 240,000, but this was not the case around the chromatographic apex of the peak (i.e. 14.05 min) (Fig. 4B, Bottom).

621

(A)

(B)

(C)
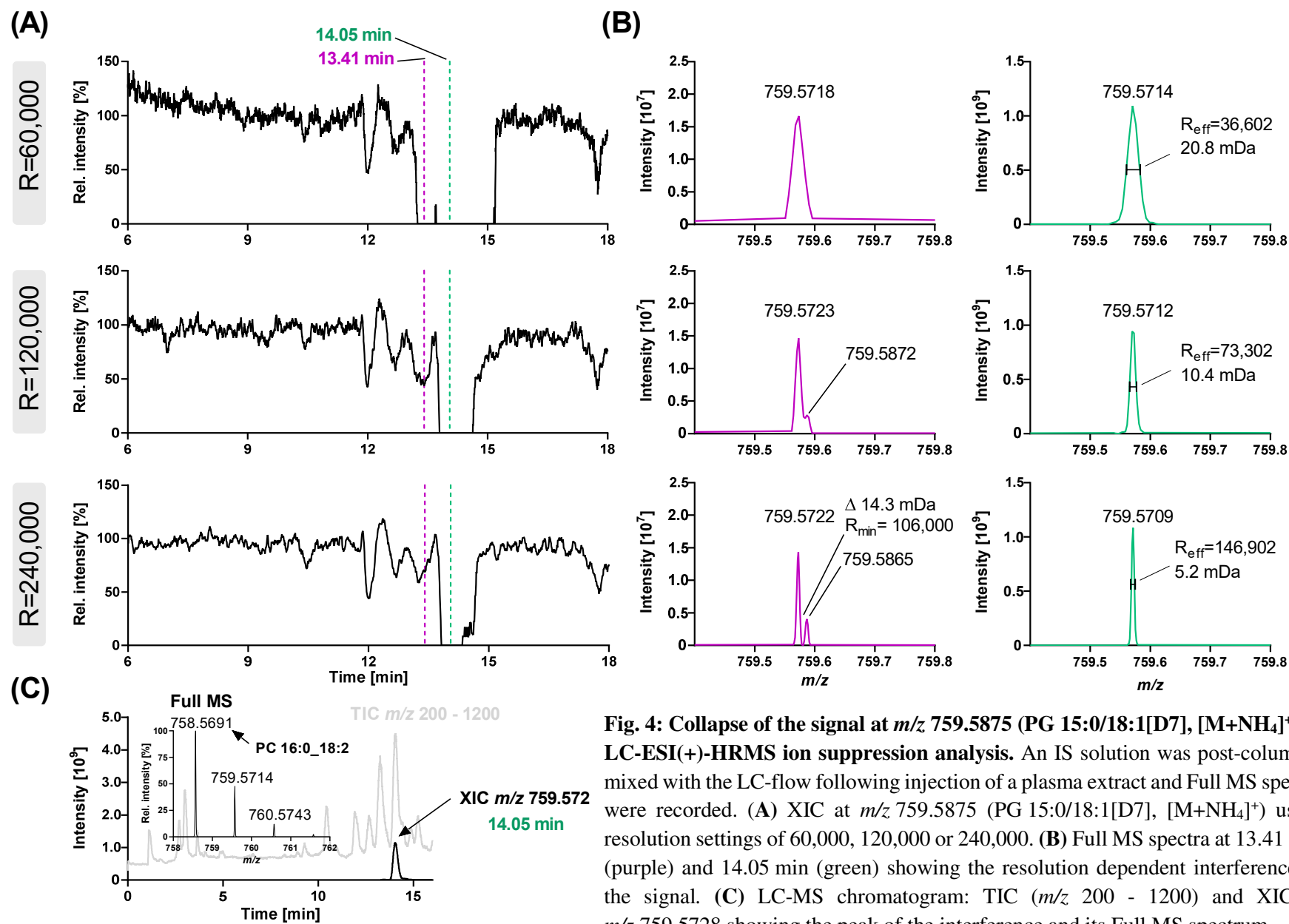
Fig. 4: Collapse of the signal at *m/z* 759.5875 (PG 15:0/18:1[D7], [M+NH₄]⁺) in LC-ESI(+)-HRMS ion suppression analysis. An IS solution was post-columnly mixed with the LC-flow following injection of a plasma extract and Full MS spectra were recorded. **(A)** XIC at *m/z* 759.5875 (PG 15:0/18:1[D7], [M+NH₄]⁺) using resolution settings of 60,000, 120,000 or 240,000. **(B)** Full MS spectra at 13.41 min (purple) and 14.05 min (green) showing the resolution dependent interference of the signal. **(C)** LC-MS chromatogram: TIC (*m/z* 200 - 1200) and XIC at *m/z* 759.5728 showing the peak of the interference and its Full MS spectrum.

Using a standard solution of PC 16:0/18:2(9Z,12Z) instead of a lipid extract for the ion suppression analysis, confirmed that the distortion of the signal of PG 15:0/18:1[D7] was caused by PC 16:0/18:2(9Z,12Z) ions at high abundance: When 6 µM of the PC 16:0/18:2(9Z,12Z) was injected the signal of PG 15:0/18:1[D7] at 14.05 min was distorted, while decreasing the injected concentration of the PC 16:0/18:2(9Z,12Z) to a similar intensity of the ions at *m/z* 759.5728 and *m/z* 759.5875 allowed the parallel detection of both *m/z* (Fig. S5). The distortion of the *m/z* also depended on the amount of ions and the filling of the orbitrap (defined by the AGC target): When the ratio of PC 16:0_18:2 : PG 15:0/18:1[D7] was kept constant (12 : 1), at high concentration (3-6 µM) and a high numbers of ions in the trap (AGC $\geq$ 1 x 10^6) leads again to the distortion of the signal of PG 15:0/18:1[D7]. At a lower filling of the trap (AGC target 2 x 10^4) both *m/z* were detected. In contrast, at low concentration (0.6 µM) only with a higher AGC target ($\geq$ 1 x 10^6) both *m/z* were detected (Fig. S6). Similar findings of distortion of the *m/z* signal by abundant almost isobaric ions (despite sufficient resolution) have already been reported in orbitrap MS and can be explained by the formation of ion clouds with almost identical *m/z* within the trap resulting in peak coalescence (47) Overall, this shows that using an orbitrap mass analyzer abundant lipid species influence the detection of lower abundant ones which should be considered during method development, i.e. choosing the highest resolution possible for Full MS analysis, and (ii) using an efficient chromatographic separation – as described herein – to separate almost isobaric lipids.

Overall, the LLE with MeOH/MTBE yielded excellent extraction recoveries of the lysophospholipids and phospholipids, and apparent losses resulted mainly from ion suppression. 10 µL of plasma were chosen for LLE to limit matrix effects and to enable semi-quantification. Intra- and inter-day variance <100 ± 20%, as well as inter-operator variance <100 ± 18% (except for PS and PG) using different pools of plasma demonstrate the reproducibility and robustness of the extraction method underlining its suitability for lipidomics analysis (Fig. S3). The observed signal erase for PG due to the [^{13}C$_1$] of PC 16:0_18:2 in ESI(+) does not impact the detection of PG 15:0/18:1[D7] because it elutes earlier at 11.43 min (Table 1). However, it should be kept in mind that the detection of lipid species with nearly identical *m/z* eluting at the same time might be disturbed using FT-MS instruments resulting in loss or distortion of information regarding their presence. This is particularly an issue in shotgun

650 analysis where all ions enter the MS at the same time but also might occur to some extent when

651 combined with chromatographic separation. The use of a higher resolution might reduce this effect but

652 cannot prevent deletion of the signal of minor lipid species by dominating ions with similar *m/z*.

653 Application: Analysis of the effects of n3-PUFA supplementation on the human plasma lipidome

654 The effects of 12 months n3-PUFA supplementation (corresponding to 4 portions of fatty fish

655 per week) on the plasma phospholipid pattern in healthy subjects were investigated aiming to

656 characterize which phospholipids are changing most following supplementation. After manual review

657 of the feature assignment by MS-DIAL, 1399 features in ESI(+) and 580 in ESI(-) were found and

658 evaluated by means of volcano plots (Fig. 5A). For evaluation which lipid species showed a relevant

659 change after n3-PUFA supplementation only features with a -log10 (*p*-value) ≥1.303 (corresponding to

660 -log10 ($p \leq 0.05$)) and a log2 (fold change) ≥0.5 or ≤-0.5 were further investigated (348 features in ESI(+)

661 and 151 in ESI(-)).

662 From these, only the features detected in both ionization modes were semi-quantified aiming

663 to i) characterize the lipid class and the fatty acyl chains of the lipids, which was not done in previous

664 lipidomics studies investigating n3-PUFA supplementation (45, 46, 48), and to ii) provide additional

665 confidence regarding the tentative identification of the lipid species and their modulation following n3-

666 PUFA supplementation by comparing the results from both ionization modes. Thus, DG, TG and Chol

667 Ester were not further evaluated (Fig. 5A). Further confidence of the lipid identification was obtained

668 utilizing retention time behavior of lipids in RPLC which correlates with the equivalent carbon number.

669 Plotting the retention times of the lipid species *vs.* the carbon number of the fatty acyl chains (Fig. S9)

670 or *vs.* the number of double bonds (Fig. S10) showed good correlation of polynomial regression for the

671 different lipid classes (12). A total of 98 lipid species were semi-quantified based on their peak height

672 using the IS of the same lipid class and concentrations obtained in ESI(+) and ESI(-) mode were

673 comparable (Table S5). For the TOP 5 most changing lipids (relatively and absolutely) (Fig. 5C-D),

674 additionally the concentrations for each subject are given in the supplementary material (Table S6).

675
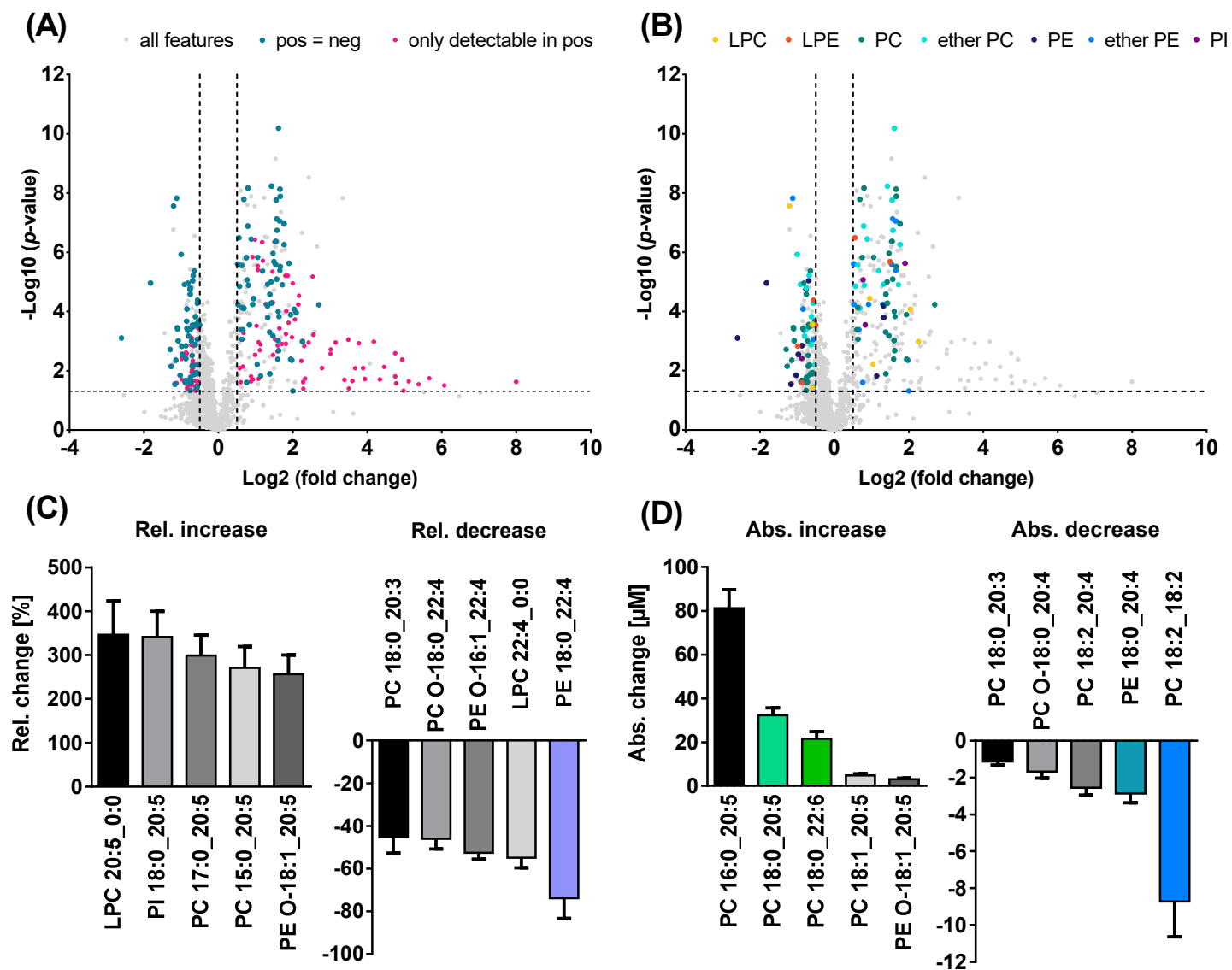
Fig. 5: Untargeted LC-HRMS analysis of human plasma following n3-PUFA supplementation. Plasma lipid extracts at baseline and following 12 months of n3-PUFA supplementation were analyzed by untargeted LC-HRMS. (**A**) Shown are volcano plots highlighting significantly changing features detected in both ionization modes and those only detectable in ESI(+). (**B**) Significantly changing features detected in both modes are highlighted according to their lipid class. Shown are the (**C**) relative and (**D**) absolute changes observed in ESI(+) for the TOP 5 most changing tentatively identified lipids (mean ± SEM, n=20). Highlighted lipids were quantified by targeted LC-MS/MS.

676   Significant changes following n3-PUFA supplementation were observed for PC, ether PC, ether

677   PE, PE, LPE, PI and LPC lipid species. With 34 lipids, most changes were observed for the PC lipid

678   class followed by ether PC, ether PE and PE with 24, 15 and 11 species, respectively (Fig. 5B).

679   Following n3-PUFA supplementation, 8 PE species decreased, while 11 ether PE species increased.

680   The change of a higher number of PC species is likely related to the high abundance of PC in human

681   plasma being the most abundant class of phospholipids accounting for around 18% of all lipids (49, 50).

682   This is in line with an earlier analysis of the samples from the same study where Browning et al. also

683   found the strongest increase of DHA+EPA in the PC fraction among the different analyzed plasma lipid

684   fractions (i.e. PC, Chol Ester and TG). However, other phospholipid classes were not analyzed (28).

685   Following n3-PUFA supplementation, the most increasing lipids bear 20:5 (Fig. 5C). It should

686   be noted that the baseline concentration of lipids bearing 20:5 was lower than of lipids bearing 22:6,

687   which is consistent with a previous study reporting a lower total fatty acid level of

688   20:5(5Z,8Z,11Z,14Z,17Z) compared to 22:6(4Z,7Z,10Z,13Z,16Z,19Z) (40 ± 28 µM and 89 ± 37 µM,

689   respectively) in plasma from healthy Canadian adults (51). Due to their lower baseline concentration, a

690   stronger increase was observed for lipids bearing 20:5: For example, LPC 20:5_0:0 was less abundant

691   at baseline than LPC 22:6_0:0 (i.e. 0.25 ± 0.11 µM *vs.* 0.80 ± 0.28 µM), and was relatively increased

692   by 350%, while LPC 22:6_0:0 showed an increase of 100%. Similar results were also observed for other

693   phospholipid classes, i.e. for the pairs PI 18:0_20:5/PI 18:0_22:6, PC 17:0_20:5/PC 17:0_22:6, LPE

694   20:5_0:0/LPE 22:6_0:0 and PC O-18:1_20:5/PC O-18:1_22:6. These observations are in line with

695   results from the same trial showing that the fatty acid 20:5(5Z,8Z,11Z,14Z,17Z) (52) and its oxylipin

696   products (e.g. 14(15)-EpETE) (53) are relatively more affected by n3-PUFA supplementation compared

697   to 22:6(4Z,7Z,10Z,13Z,16Z,19Z) and its oxylipin products. Our results are consistent with previous

698   lipidomics studies showing that LPC 20:5_0:0 increased more than LPC 22:6_0:0 following n3-PUFA

699   supplementation (45, 46). Interestingly, also the determined relative changes for LPC 20:5_0:0 (i.e.

700   4.10 *vs.* 4.35) and LPC 22:6_0:0 (i.e. 1.93 *vs.* 1.89) were similar with the studies from Ottestad et al.

701   where healthy subjects (n=16) received fish oil capsules containing 0.7 g EPA + 0.9 g DHA per day for

702   7 weeks, indicating a steady state of modulation (46).

703 The strongest relative decrease was observed for lipids bearing 22:4 with e.g. PE 18:0_22:4

704 showing a decrease of -74% and LPC 22:4_0:0 of -55% (Fig. 5C); and those bearing 20:3 with e.g. PC

705 18:0_20:3 decreasing by -45%. Other lipids bearing potential n6-PUFA, such as ARA

706 (20:4(5Z,8Z,11Z,14Z)) or linoleic acid (18:2(9Z,12Z)), also decreased following n3-PUFA

707 supplementation, e.g. PE 18:0_20:4 with -37% and PC 18:2_18:2 with -27%. Interestingly, the latter

708 showed also the strongest decrease in concentration (Fig. 5D). These results are in line with previous

709 studies reporting that n3-PUFA supplementation led to a decrease of the n6-PUFA content (28, 52, 54,

710 55). Our results are also consistent with the study from Uhl et al. where a significant decrease was found

711 for PC 16:0/22:4, PC 18:0/22:4 and PC 18:1/20:4 in plasma from subjects supplemented with

712 510 mg/day of DHA for 29 days by means of targeted lipidomics analysis (56).

713

714 **Table 4: Concentration of selected phospholipids determined by untargeted and targeted analysis**
715 **in plasma at baseline and following 12 months of n3-PUFA supplementation.** Plasma lipid extracts
716 were analyzed by untargeted LC-HRMS in both ionization modes and lipids were semi-quantified based
717 on normalized peak heights using one IS per lipid class. For quantification, extracts were analyzed by
718 targeted LC-ESI(-)-MS/MS and lipids were quantified by external calibration based on analyte to
719 corresponding IS peak area ratios. Shown are mean values ± SD, n=20.

720

		concentration [µM]					
		baseline			12 months		
		LC-ESI(+)-HRMS	LC-ESI(-)-HRMS	LC-ESI(-)-MS/MS	LC-ESI(+)-HRMS	LC-ESI(-)-HRMS	LC-ESI(-)-MS/MS
	increasing lipids						
LPC	LPC 20:5_0:0	0.25 ± 0.11	0.37 ± 0.15	-	1.0 ± 0.74	1.4 ± 0.93	-
PI	PI 18:0_20:5	0.22 ± 0.11	0.14 ± 0.061	-	0.83 ± 0.42	0.42 ± 0.18	-
PC	PC 15:0_20:5	0.19 ± 0.084	0.37 ± 0.15	-	0.61 ± 0.27	1.1 ± 0.41	-
	PC 16:0_20:5	38 ± 18	51 ± 21	-	119 ± 42	134 ± 39	-
	PC 17:0_20:5	0.34 ± 0.14	0.51 ± 0.21	-	1.2 ± 0.44	1.7 ± 0.51	-
	PC 18:0/20:5(5Z,8Z,11Z,14Z,17Z)	15 ± 6.5	20 ± 8.1	17 ± 7.2	47 ± 16	55 ± 16	56 ± 19
	PC 18:1_20:5	2.8 ± 1.3	4.4 ± 1.8	-	7.6 ± 4.3	11 ± 4.7	-
	PC 18:0/22:6(4Z,7Z,10Z,13Z,16Z,19Z)	32 ± 12	34 ± 11	51 ± 17	54 ± 14	53 ± 15	90 ± 28
Ether PE	PE O-18:1_20:5	1.6 ± 0.95	1.3 ± 0.72		4.7 ± 2.3	3.9 ± 1.8	-
	decreasing lipids						
LPC	LPC 22:4_0:0	0.058 ± 0.020	0.078 ± 0.028	-	0.025 ± 0.012	0.034 ± 0.017	-
PC	PC 18:0_20:3	2.4 ± 1.9	3.1 ± 2.3	-	0.98 ± 0.51	1.4 ± 0.67	-
	PC 18:2_20:4	7.0 ± 2.0	11 ± 2.5	-	4.5 ± 1.2	6.8 ± 1.4	-
	PC 18:2(9Z,12Z)/18:2(9Z,12Z)	28 ± 10	37 ± 12	15 ± 4.9	19 ± 7.0	25 ± 7.8	10 ± 3.4
PE	**PE 18:0/20:4(5Z,8Z,11Z,14Z)**	6.9 ± 2.5	7.4 ± 2.7	11 ± 4.1	4.1 ± 1.1	4.8 ± 1.5	7.4 ± 2.1
	PE 18:0/22:4(7Z,10Z,13Z,16Z)	0.19 ± 0.17	0.18 ± 0.14	0.12 ± 0.091	0.030 ± 0.043	0.050 ± 0.038	0.041 ± 0.025
Ether PC	PC O-18:0_20:4	4.8 ± 1.6	5.8 ± 1.5	-	3.1 ± 1.1	3.7 ± 1.2	-
	PC O-18:0_22:4	0.61 ± 0.20	0.81 ± 0.20	-	0.30 ± 0.093	0.36 ± 0.13	-
Ether PE	PE O-16:1_22:4	0.47 ± 0.15	0.31 ± 0.094	-	0.22 ± 0.067	0.17 ± 0.045	-

730

731

732

733   In order to support the results determined with the untargeted approach, several of the most

734 changing phospholipids in the plasma were quantified using targeted LC-MS/MS. Targeted analysis

735 confirmed the tentative identification of the phospholipids PC 18:0/20:5(5Z,8Z,11Z,14Z,17Z), PC

736 18:0/22:6(4Z,7Z,10Z,13Z,16Z,19Z), PE 18:0/20:4(5Z,8Z,11Z,14Z), PE 18:0/22:4(7Z,10Z,13Z,16Z)

737 and PC 18:2(9Z,12Z)/18:2(9Z,12Z) (Table 4, Fig. S11). Concentrations determined by quantitative

738 targeted LC-MS/MS were in the same range as those semi-quantified by means of LC-HRMS, also

739 confirming the observed increase and decrease following n3-PUFA supplementation (Fig. 6).

740 Quantitative targeted analysis resulted in almost same concentration for PC

741 18:0/20:5(5Z,8Z,11Z,14Z,17Z), while <2.5 fold difference in concentrations were found for PC

742 18:0/22:6(4Z,7Z,10Z,13Z,16Z,19Z), PE 18:0/20:4(5Z,8Z,11Z,14Z), PE 18:0/22:4(7Z,10Z,13Z,16Z)

743 and PC 18:2(9Z,12Z)/18:2(9Z,12Z).
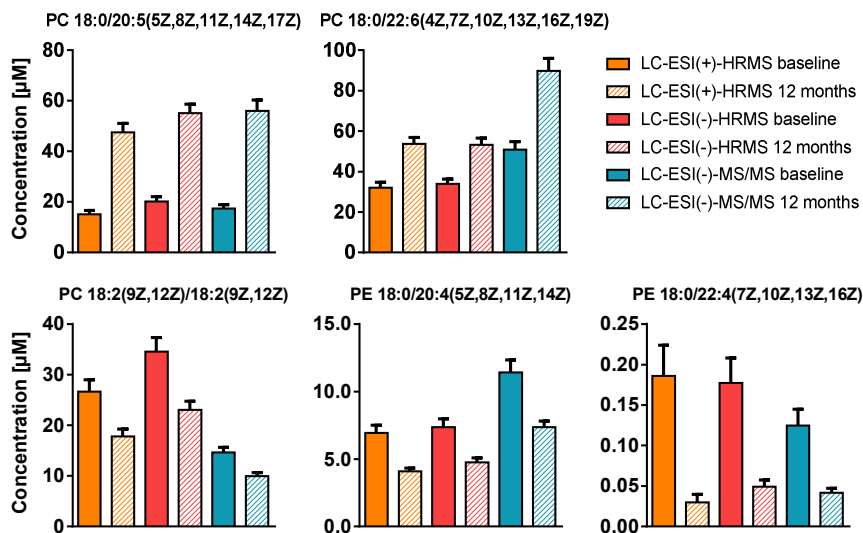
744 **Fig. 6: Comparison of concentrations of selected phospholipids determined by means of**
745 **untargeted LC-HRMS and targeted LC-MS/MS.** Plasma lipid extracts were analyzed by untargeted
746 LC-HRMS and lipids were semi-quantified based on peak heights using one IS per lipid class. For
747 quantification, the extracts were analyzed by targeted LC-ESI(-)-MS/MS and lipids were quantified by
748 external calibration based on analyte to corresponding IS peak area ratios. Shown are the concentrations
749 of selected phospholipids at baseline and following 12 months of supplementation (mean ± SEM, n=20).

750   This supports the suitability of the developed untargeted LC-HRMS method to monitor changes

751 in the phospholipid pattern in plasma. Our results showed a significant increase of lipids bearing n3-

752 PUFA combined with a decrease of lipids bearing n6-PUFA (28, 52, 54). PC

753 18:0/20:5(5Z,8Z,11Z,14Z,17Z) and PC 18:2(9Z,12Z)/18:2(9Z,12Z) were found to be significantly

754 modulated and might be further investigated as possible biomarker for n3-PUFA consumption.

Conclusion

We optimized and characterized the performance of an LC-HRMS method for the semi-quantification of polar lipids in human plasma. Individual MS parameters were systematically optimized allowing a threefold gain in sensitivity. It was shown that the setting of the auxiliary gas is critical for the spray stability and the S-lens RF level has a relevant impact on the ion transmission and signal intensity. Optimization of chromatographic parameters showed that the selection of the RP C18 column has a great impact on the separation efficiency and peak shape, indicating that surface interactions play a relevant role on phospholipid separation in RPLC.

Data-dependent MS^2 settings were identified to be crucial and the number of TOP N was adjusted based on the FWHM of the chromatographic peaks over the elution time in a staggered manner. This allows the acquisition of as many meaningful MS^2 spectra as possible for lipid characterization, while recording enough data points across the peaks for semi-quantification. Of note, we found that high abundant lipids can distort the detection of lipids with similar *m/z* in the orbitrap mass analyzer. Thus, the highest resolution possible should be selected for Full MS analysis, however this does not resolve the problem completely.

Thorough characterization of matrix effects by pre and post extraction spiking, as well as ion suppression analysis of plasma unveiled that apparent losses are caused by ion suppression. Thus, concentrations resulting from semi-quantification based on only one IS per lipid class might be affected by coeluting interferences in RPLC. However, determined concentrations in plasma by untargeted LC-HRMS were comparable in ESI(-) and ESI(+), and in the same range as those obtained by targeted LC-MS/MS.

The developed LC-HRMS method was successfully used to investigate the effects of n3-PUFA supplementation on the phospholipid pattern in human plasma. A total of 98 phospholipids significantly changed after supplementation were semi-quantified in both ionization modes. A strong increase was found for lipids bearing 20:5, while lipids bearing 22:4, and of note PC 18:2(9Z,12Z)/18:2(9Z,12Z) were lowered. Quantitative targeted analysis confirmed the identification of selected phospholipids and their relative change following n3-PUFA supplementation. The concentration difference between the

782 targeted and the untargeted approach was less than 2.5 fold, underlying the reliability of the semi-

783 quantification using the developed untargeted LC-HRMS method.

784

785 **References**

786 1.   Fahy E, Subramaniam S, Brown HA, Glass CK, Merrill AH, Murphy RC, et al. A comprehensive
787 classification system for lipids1. Journal of lipid research. 2005;46(5):839-61.

788 2.   Calder PC. Functional roles of fatty acids and their effects on human health. Journal of
789 parenteral and enteral nutrition. 2015;39:18S-32S.

790 3.   Li J, Wang X, Zhang T, Wang C, Huang Z, Luo X, et al. A review on phospholipids and their
791 main applications in drug delivery systems. Asian journal of pharmaceutical sciences. 2015;10(2):81-
792 98.

793 4.   Van Meer G, Voelker DR, Feigenson GW. Membrane lipids: where they are and how they
794 behave. Nature reviews Molecular cell biology. 2008;9(2):112-24.

795 5.   Bird SS, Marur VR, Stavrovskaya IG, Kristal BS. Separation of cis–trans phospholipid isomers
796 using reversed phase LC with high resolution MS detection. Analytical chemistry. 2012;84(13):5509-
797 17.

798 6.   Cajka T, Fiehn O. Comprehensive analysis of lipids in biological systems by liquid
799 chromatography-mass spectrometry. TrAC Trends in Analytical Chemistry. 2014;61:192-206.

800 7.   Hu C, Zhou Y, Feng J, Zhou S, Li C, Zhao S, et al. Untargeted lipidomics reveals specific lipid
801 abnormalities in nonfunctioning human pituitary adenomas. Journal of proteome research.
802 2019;19(1):455-63.

803 8.   Khan MJ, Codreanu SG, Goyal S, Wages PA, Gorti SK, Pearson MJ, et al. Evaluating a targeted
804 multiple reaction monitoring approach to global untargeted lipidomic analyses of human plasma.
805 Rapid Communications in Mass Spectrometry. 2020;34(22):e8911.

806 9.   Shan J, Qian W, Kang A, Peng L, Xie T, Lin L, et al. Lipid profile perturbations in the plasma
807 and lungs of mice with LPS-induced acute lung injury revealed by UHPLC-ESI-Q Exactive HF MS
808 analysis. Journal of pharmaceutical and biomedical analysis. 2019;162:242-8.

809 10.   Narváez-Rivas M, Zhang Q. Comprehensive untargeted lipidomic analysis using core–shell
810 C30 particle column and high field orbitrap mass spectrometer. Journal of Chromatography A.
811 2016;1440:123-34.

812 11.   Criscuolo A, Zeller M, Cook K, Angelidou G, Fedorova M. Rational selection of reverse phase
813 columns for high throughput LC–MS lipidomics. Chemistry and physics of lipids. 2019;221:120-7.

814 12.   Vaňková Z, Peterka O, Chocholoušková M, Wolrab D, Jirásko R, Holčapek M. Retention
815 dependences support highly confident identification of lipid species in human plasma by reversed-
816 phase UHPLC/MS. Analytical and Bioanalytical Chemistry. 2022:1-13.

817 13.   Damen CW, Isaac G, Langridge J, Hankemeier T, Vreeken RJ. Enhanced lipid isomer
818 separation in human plasma using reversed-phase UPLC with ion-mobility/high-resolution MS
819 detection [S]. Journal of lipid research. 2014;55(8):1772-83.

820 14.   Xu T, Hu C, Xuan Q, Xu G. Recent advances in analytical strategies for mass spectrometry-
821 based lipidomics. Analytica Chimica Acta. 2020;1137:156-69.

822 15.   Züllig T, Trötzmüller M, Köfeler HC. Lipidomics from sample preparation to data analysis: a
823 primer. Analytical and bioanalytical chemistry. 2020;412:2191-209.

824 16.   Rund KM, Ostermann AI, Kutzner L, Galano J-M, Oger C, Vigor C, et al. Development of an LC-
825 ESI (-)-MS/MS method for the simultaneous quantification of 35 isoprostanes and isofurans derived
826 from the major n3-and n6-PUFAs. Analytica chimica acta. 2018;1037:63-74.

827 17.   Hartung NM, Mainka M, Pfaff R, Kuhn M, Biernacki S, Zinnert L, et al. Development of a
828 quantitative proteomics approach for cyclooxygenases and lipoxygenases in parallel to quantitative

829 oxylipin analysis allowing the comprehensive investigation of the arachidonic acid cascade.
830 Analytical and Bioanalytical Chemistry. 2023;415(5):913-33.

831 18.   Zhou H, Nong Y, Zhu Y, Liang Y, Zhang J, Chen H, et al. Serum untargeted lipidomics by
832 UHPLC-ESI-HRMS aids the biomarker discovery of colorectal adenoma. BMC cancer. 2022;22(1):1-14.

833 19.   Gil A, Zhang W, Wolters JC, Permentier H, Boer T, Horvatovich P, et al. One-vs two-phase
834 extraction: re-evaluation of sample preparation procedures for untargeted lipidomics in plasma
835 samples. Analytical and Bioanalytical Chemistry. 2018;410:5859-70.

836 20.   Lee H-C, Yokomizo T. Applications of mass spectrometry-based targeted and non-targeted
837 lipidomics. Biochemical and biophysical research communications. 2018;504(3):576-81.

838 21.   Wolrab D, Chocholoušková M, Jirásko R, Peterka O, Holčapek M. Validation of lipidomic
839 analysis of human plasma and serum by supercritical fluid chromatography–mass spectrometry and
840 hydrophilic interaction liquid chromatography–mass spectrometry. Analytical and bioanalytical
841 chemistry. 2020;412:2375-88.

842 22.   Koch E, Mainka M, Dalle C, Ostermann AI, Rund KM, Kutzner L, et al. Stability of oxylipins
843 during plasma generation and long-term storage. Talanta. 2020;217:121074.

844 23.   Matyash V, Liebisch G, Kurzchalia TV, Shevchenko A, Schwudke D. Lipid extraction by methyl-
845 tert-butyl ether for high-throughput lipidomics. Journal of lipid research. 2008;49(5):1137-46.

846 24.   Ostermann AI, Koch E, Rund KM, Kutzner L, Mainka M, Schebb NH. Targeting esterified
847 oxylipins by LC–MS-Effect of sample preparation on oxylipin pattern. Prostaglandins & Other Lipid
848 Mediators. 2020;146:106384.

849 25.   Meckelmann SW, Hawksworth JI, White D, Andrews R, Rodrigues P, O'Connor A, et al.
850 Metabolic dysregulation of the lysophospholipid/autotaxin axis in the chromosome 9p21 gene SNP
851 rs10757274. Circulation: Genomic and Precision Medicine. 2020;13(3):e002806.

852 26.   Bligh EG, Dyer WJ. A rapid method of total lipid extraction and purification. Canadian journal
853 of biochemistry and physiology. 1959;37(8):911-7.

854 27.   Hara A, Radin NS. Lipid extraction of tissues with a low-toxicity solvent. Analytical
855 biochemistry. 1978;90(1):420-6.

856 28.   Browning LM, Walker CG, Mander AP, West AL, Madden J, Gambell JM, et al. Incorporation
857 of eicosapentaenoic and docosahexaenoic acids into lipid pools when given as supplements
858 providing doses equivalent to typical intakes of oily fish. The American journal of clinical nutrition.
859 2012;96(4):748-58.

860 29.   Tsugawa H, Cajka T, Kind T, Ma Y, Higgins B, Ikeda K, et al. MS-DIAL: data-independent
861 MS/MS deconvolution for comprehensive metabolome analysis. Nature methods. 2015;12(6):523-6.

862 30.   Pi J, Wu X, Feng Y. Fragmentation patterns of five types of phospholipids by ultra-high-
863 performance liquid chromatography electrospray ionization quadrupole time-of-flight tandem mass
864 spectrometry. Analytical methods. 2016;8(6):1319-32.

865 31.   Liebisch G, Fahy E, Aoki J, Dennis EA, Durand T, Ejsing CS, et al. Update on LIPID MAPS
866 classification, nomenclature, and shorthand notation for MS-derived lipid structures. Journal of lipid
867 research. 2020;61(12):1539-55.

868 32.   Bird SS, Marur VR, Sniatynski MJ, Greenberg HK, Kristal BS. Serum lipidomics profiling using
869 LC–MS and high-energy collisional dissociation fragmentation: focus on triglyceride detection and
870 characterization. Analytical chemistry. 2011;83(17):6648-57.

871 33.   Kiyonami R, Peake D, Huang Y. Increased identification coverage and throughput for
872 complex lipidomes. Thermo Fisher Scientific Application Note. 2016;607.

873 34.   Chen W, Zeng J, Wang W, Yang B, Zhong L, Zhou J. Comprehensive metabolomic and
874 lipidomic analysis reveals metabolic changes after mindfulness training. Mindfulness.
875 2020;11(6):1390-400.

876 35.   Xu X, Luo Z, He Y, Shan J, Guo J, Li J. Application of untargeted lipidomics based on UHPLC-
877 high resolution tandem MS analysis to profile the lipid metabolic disturbances in the heart of
878 diabetic cardiomyopathy mice. Journal of Pharmaceutical and Biomedical Analysis.
879 2020;190:113525.

36.   Gallart-Ayala H, Courant F, Severe S, Antignac J-P, Morio F, Abadie J, et al. Versatile lipid profiling by liquid chromatography–high resolution mass spectrometry using all ion fragmentation and polarity switching. Preliminary application for serum samples phenotyping related to canine mammary cancer. Analytica chimica acta. 2013;796:75-83.

37.   Forest A, Ruiz M, Bouchard B, Boucher G, Gingras O, Daneault C, et al. Comprehensive and reproducible untargeted lipidomic workflow using LC-QTOF validated for human plasma analysis. Journal of proteome research. 2018;17(11):3657-70.

38.   Géhin C, Fowler SJ, Trivedi DK. Chewing the fat: How lipidomics is changing our understanding of human health and disease in 2022. Analytical Science Advances. 2023.

39.   Hutchins PD, Russell JD, Coon JJ. Accelerating lipidomic method development through in silico simulation. Analytical chemistry. 2019;91(15):9698-706.

40.   Ogiso H, Suzuki T, Taguchi R. Development of a reverse-phase liquid chromatography electrospray ionization mass spectrometry method for lipidomics, improving detection of phosphatidic acid and phosphatidylserine. Analytical biochemistry. 2008;375(1):124-31.

41.   Schwaiger M, Schoeny H, El Abiead Y, Hermann G, Rampler E, Koellensperger G. Merging metabolomics and lipidomics into one analytical run. Analyst. 2019;144(1):220-9.

42.   Zhou J, Sun L, Chen L, Liu S, Zhong L, Cui M. Comprehensive metabolomic and proteomic analyses reveal candidate biomarkers and related metabolic networks in atrial fibrillation. Metabolomics. 2019;15(7):1-13.

43.   Wong MWK, Braidy N, Pickford R, Sachdev PS, Poljak A. Comparison of single phase and biphasic extraction protocols for lipidomic studies using human plasma. Frontiers in neurology. 2019;10:879.

44.   Wang B, Tontonoz P. Phospholipid remodeling in physiology and disease. Annual review of physiology. 2019;81:165-88.

45.   Yan M, Cai WB, Hua T, Cheng Q, Ai D, Jiang HF, et al. Lipidomics reveals the dynamics of lipid profile altered by omega-3 polyunsaturated fatty acid supplementation in healthy people. Clinical and Experimental Pharmacology and Physiology. 2020;47(7):1134-44.

46.   Ottestad I, Hassani S, Borge GI, Kohler A, Vogt G, Hyötyläinen T, et al. Fish oil supplementation alters the plasma lipidomic profile and increases long-chain PUFAs of phospholipids and triglycerides in healthy subjects. 2012.

47.   Gorshkov MV, Fornelli L, Tsybin YO. Observation of ion coalescence in Orbitrap Fourier transform mass spectrometry. Rapid Communications in Mass Spectrometry. 2012;26(15):1711-7.

48.   Lankinen M, Schwab U, Erkkilä A, Seppänen-Laakso T, Hannila M-L, Mussalo H, et al. Fatty fish intake decreases lipids related to inflammation and insulin signaling—a lipidomics approach. PLoS one. 2009;4(4):e5258.

49.   Bowden JA, Heckert A, Ulmer CZ, Jones CM, Koelmel JP, Abdullah L, et al. Harmonizing lipidomics: NIST interlaboratory comparison exercise for lipidomics using SRM 1950–Metabolites in Frozen Human Plasma [S]. Journal of lipid research. 2017;58(12):2275-88.

50.   Burla B, Arita M, Arita M, Bendt AK, Cazenave-Gassiot A, Dennis EA, et al. Ms-based lipidomics of human blood plasma: A community-initiated position paper to develop accepted guidelines1. Journal of lipid research. 2018;59(10):2001-17.

51.   Abdelmagid SA, Clarke SE, Nielsen DE, Badawi A, El-Sohemy A, Mutch DM, et al. Comprehensive profiling of plasma fatty acid concentrations in young healthy Canadian adults. PloS one. 2015;10(2):e0116195.

52.   Dawczynski C, Massey KA, Ness C, Kiehntopf M, Stepanow S, Platzer M, et al. Randomized placebo-controlled intervention with n-3 LC-PUFA-supplemented yoghurt: effects on circulating eicosanoids and cardiovascular risk factors. Clinical nutrition. 2013;32(5):686-96.

53.   Ostermann AI, West AL, Schoenfeld K, Browning LM, Walker CG, Jebb SA, et al. Plasma oxylipins respond in a linear dose-response manner with increased intake of EPA and DHA: results from a randomized controlled trial in healthy humans. The American journal of clinical nutrition. 2019;109(5):1251-63.

931 54.   Schuchardt JP, Ostermann AI, Stork L, Kutzner L, Kohrs H, Greupner T, et al. Effects of
932 docosahexaenoic acid supplementation on PUFA levels in red blood cells and plasma. Prostaglandins,
933 Leukotrienes and Essential Fatty Acids. 2016;115:12-23.
934 55.   Walker CG, West AL, Browning LM, Madden J, Gambell JM, Jebb SA, et al. The pattern of
935 fatty acids displaced by EPA and DHA following 12 months supplementation varies between blood
936 cell and plasma fractions. Nutrients. 2015;7(8):6281-93.
937 56.   Uhl O, Demmelmair H, Klingler M, Koletzko B. Changes of molecular glycerophospholipid
938 species in plasma and red blood cells during docosahexaenoic acid supplementation. Lipids.
939 2013;48(11):1103-13.

940

941